Table 1
Body weight change after inoculation of various vaccines

Biological name	N	Body weight change after inoculation							
		Day 1		Day 2		Day 3		Day 4	
		AVE	VAR	AVE	VAR	AVE	VAR	AVE	VAR
Control (non-treatment, NT)	138	2.065	40.777	11.261	43.056	19.355	61.807	52.297	175.145
Control (saline, SA)	68	−2.382	23.046	8.544	35.714	16.176	36.386	48.456	147.326
Influenza HA vaccine (Flu-HA)	460	−5.098	59.160	8.148	63.372	16.467	65.914	52.507	173.819
Adsorbed diphtheria-purified pertussis–tetanus combined vaccine (DPT)	274	−4.704	40.495	6.215	44.199	14.712	61.898	47.588	179.100
Japanese encephalitis vaccine (JEV)	248	−9.734	45.370	6.520	46.639	15.210	47.470	47.895	148.119
Adsorbed hepatitis B vaccine (CHO) (HBV)	81	−6.074	27.119	6.568	35.248	14.074	62.519	50.235	168.307
Adsorbed tetanus toxoid (ATT)	79	−3.633	51.671	7.544	68.636	15.759	88.236	49.595	200.039
Adsorbed diphtheria–tetanus Combined Toxoid (ADCT)	55	−6.164	54.325	4.709	53.877	14.218	69.433	47.545	192.808
Pneumococcal vaccine polyvalent (PVP)	48	−38.813	65.092	−44.375	90.282	−27.021	97.340	21.667	101.163
Cholera vaccine (CV)	44	−14.568	79.879	−3.045	106.789	6.227	54.087	38.000	179.349
Freeze-dried inactivated tissue culture rabies vaccine (RV)	29	−11.241	40.047	4.276	68.778	12.448	68.399	43.345	105.448
Freeze-dried inactivated tissue culture hepatitis A vaccine (HAV)	28	−0.964	58.554	9.107	39.284	14.357	38.608	47.321	142.078
Yellow fever vaccine (YFV)	12	−1.000	24.545	10.917	24.992	18.500	47.364	55.417	142.629
Well's disease and Akiyami combined vaccine (WDACV)	12	−15.083	85.174	−7.750	171.477	2.917	101.902	37.583	341.174
Adsorbed habu-venom toxoid (HT)	10	−7.000	33.333	3.800	22.400	10.700	23.789	40.500	134.722
Adsorbed diphtheria toxoid for adult use (ADT)	8	−12.750	36.500	−0.375	42.554	7.250	42.214	47.000	143.143
Freeze-dried mamushi antivenom, equine (MA)	6	−1.500	16.300	6.667	47.867	14.500	30.300	51.833	224.967
Freeze-dried habu antivenom, equine (HA)	6	2.500	14.300	14.167	116.167	25.833	198.167	55.667	435.067
Freeze-dried botulism antitoxin, equine (BA)	4	1.500	13.667	12.000	22.000	18.750	18.917	56.250	47.583
Freeze-dried gas gangrene Antitoxin, equine (GGA)	2	−8.000	128.000	14.500	60.500	23.000	0.000	53.500	112.500
Gas gangrene antitoxin, equine (GGAe)	2	8.000	2.000	16.000	18.000	22.500	84.500	38.500	40.500

The average (AVE) and variance (VAR) of body weight change 1, 2, 3, and 7 days after various vaccines treatment were shown.

statistical analyses, according to the MRBP in Japan [12]. To evaluate difference between clean grade and SPF grade guinea pigs, Spearman's rank correlation coefficient (r) was calculated. All statistical analyses were performed using GraphPad Prism (version 4, GraphPad Software, San Diego, CA), Excel 2008 (Microsoft Japan, Tokyo, Japan) and JMP Statistical Software (version 5, SAS Institute Inc., Cary, NC).

2.4. Histology

At day 7 after vaccination, animals were anesthetized with pentobarbital (50 mg/kg). Afterwards, pancreas, spleen and liver specimens were excised and weighed. Tissues were fixed in Bouin's solution (Sigma, St. Louis, MO) and 4% (w/v) paraformaldehyde in phosphate-buffered saline (PBS) at 4 °C for 24 h. After fixation, tissues were dehydrated through a series of graded ethanols and xylene and embedded in paraffin. Paraffin-embedded specimens were cut into 4 μm sections and stained with hematoxylin and eosin. The surface area of focal necrosis and aluminum deposition were measured using a slide gauge.

3. Results

3.1. Selection of healthy animals in the preliminary test

Prior to performing ATT, guinea pigs (280–300 g body weight) were monitored for 7 days under normal conditions (Fig. 1A). Fig. 1B shows the data of body weight change monitored for 7 days before the start of ATT, which was obtained from previous tests done in NIID using 8000 guinea pigs. As shown in Fig. 1C, the increase in body weight followed a linear regression ($Y = 14.899X - 13.054$, $R^2 = 0.9655$) and the daily increase in body weight was normally-distributed at days 2 and 3 after the animals arrived at the laboratory. Body weights were increased by 10.87 ± 6.58 g at day 2 and by a further 7.963 ± 5.51 g at day 3. Body weight changes at day 1 were highly variable due to transportation stress and dietary conditions prior to delivery. Thus, we have not taken body weight changes at day 1 into consideration (data not shown). Based on these preliminary test data above, we judged and selected animals with coefficients of regression of 5 and coefficients of correlation to the parent population of 0.866 as being suitable for further experimentation. After selection, the guinea pigs were classified according to their final body weights and randomized to different vaccine-treated groups. Vaccines was injected intra-peritoneally and body weights were monitored for the next 7 days.

3.2. Body weight changes after vaccine injection

Table 1 shows types of vaccines used in this study. We used two control groups, non-treated (NT) and saline-treated (SA) one. Fig. 2A-1 shows body weight changes after the vaccine injection over the 7 day period. In the NT group, body weight increased by 2.065 g at day 1, then by 11.261 g (day 2), 19.355 g (day 3), and 52.297 g (day 7) (Fig. 2A). In the SA group, body weight initially decreased by 2.382 g at day 1, but then increased by 8.544 g (day 2), 16.176 g (day 3), and 48.456 g (day 7) (Fig. 2B). As in the SA group, body weights

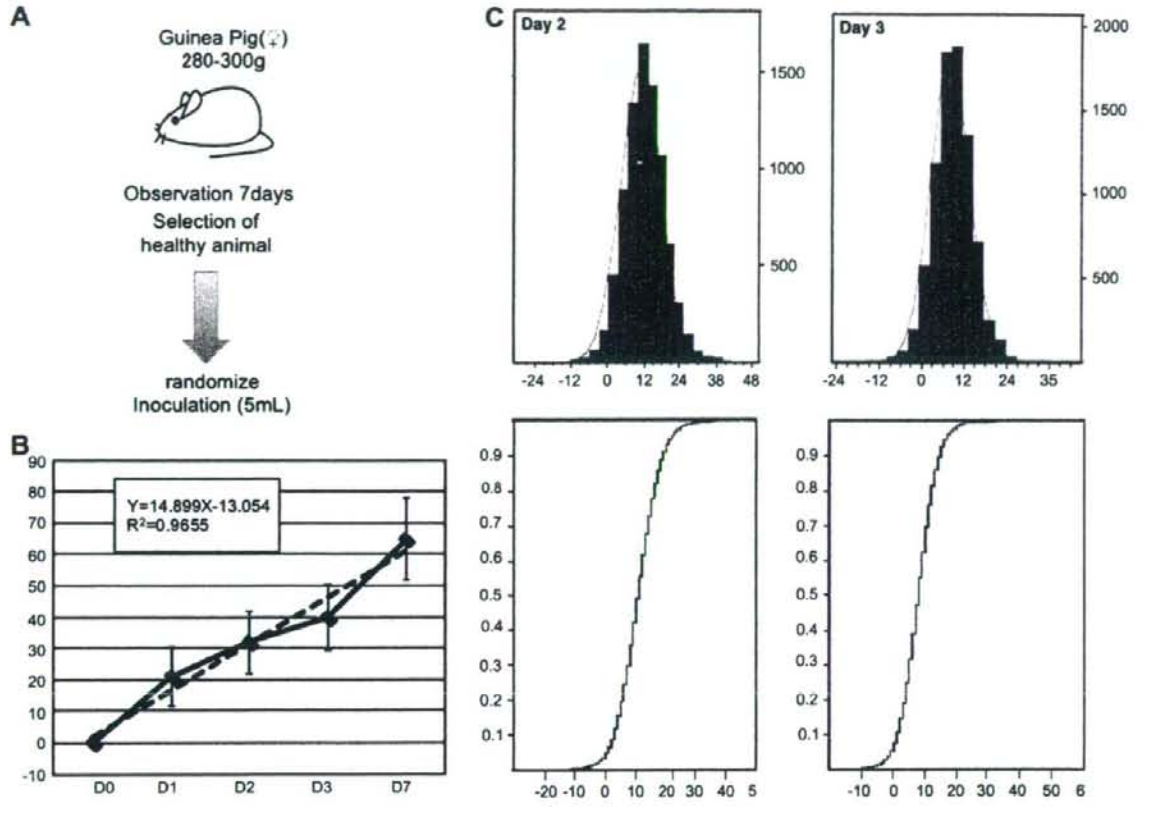

Fig. 1. Preliminary phase of abnormal toxicty test. (A) Summary of preliminary test. (B) Body weight changes after the arrival of guinea pigs at our animal facility. Collinear approximation is $Y = 14.899X - 13.054$ and coefficient of determination $R^2 = 0.9655$. (C) Upper panel: normal distribution of daily body weight change at day 2 and 3. Lower panel: cumulative distribution of daily body weight changes at day 2 and 3.

initially declined in several vaccine-treated guinea pigs: −5.098 g (influenza vaccine;; Flu-HA), −4.704 g (adsorbed diphtheria-purified pertussis−tetanus combined vaccine, DPT), −9.734 g (Japanese encephalitis vaccine, JEV), −6.074 g (recombinant adsorbed hepatitis B vaccine, HBV), −3.633 g (adsorbed tetanus toxoid, TT), −6.164 g (adsorbed diphtheria−tetanus combined vaccine, ADCT), and −38.813 g (pneumococcal vaccine polyvalent, PCV) (Fig. 2C-J). At day 2, body weights increased to reach and exceed the initial body weights in the Flu-HA-, DTP-, JEV-, HBV-, TT- and ADCT-treated guinea pigs. Body weights continued to decline at day 2 only in the PVP-treated guinea pigs (−44.375 g), and although body weights had increased by day 3, they had still not reached the initial body weight. At day 7, body weights had increased and recovered to the initial body weights in the PVP-treated guinea pigs. These trends in body weight changes followed a specific pattern with an initial reduction in body weight followed by an increase to the original body weight, with the increase being almost linear. Body weight changes at day 1 for various vaccines are summarized in Fig. 2J. Using the body weight curve data for each vaccine of at least 50 batches of vaccine, we constructed standard body weight change values for each vaccine. The population of animals with these values are known as the "reference population" (RP) (Table 1). Deviations from RP values were calculated by z-test, and if the values are within the reference range ($P < 0.01$) and no pathological signs were evident, we judged that the test specimen passed ATT. If the body weights fell below the reference values, ATT was repeated twice more before final judgment.

3.3. Pathological changes in vaccine-treated guinea pigs

Pathological changes, such as hemorrhagic ascites (Fig. 3A) and inflammation of the pancreas (Fig. 3B, C) were seen with guinea pigs receiving DPT, aluminum adsorbed vaccine and toxoid. Such changes were associated with a significant decrease of the body weight in comparison with RP ($P < 0.01$). However, the pathological effects varied among different batches of vaccines. The statistical analysis of ATT results improved the identification of pathological changes in the liver, spleen and pancreas. We measured the number of leukocytes (Fig. 3F), pancreas (Fig. 3G) and spleen weights (Fig. 3H), the area of focal necrosis in the liver (Fig. 3I) and the area of aluminum deposition in the pancreas (Fig. 3J), using more than 10 batches of each vaccine. These

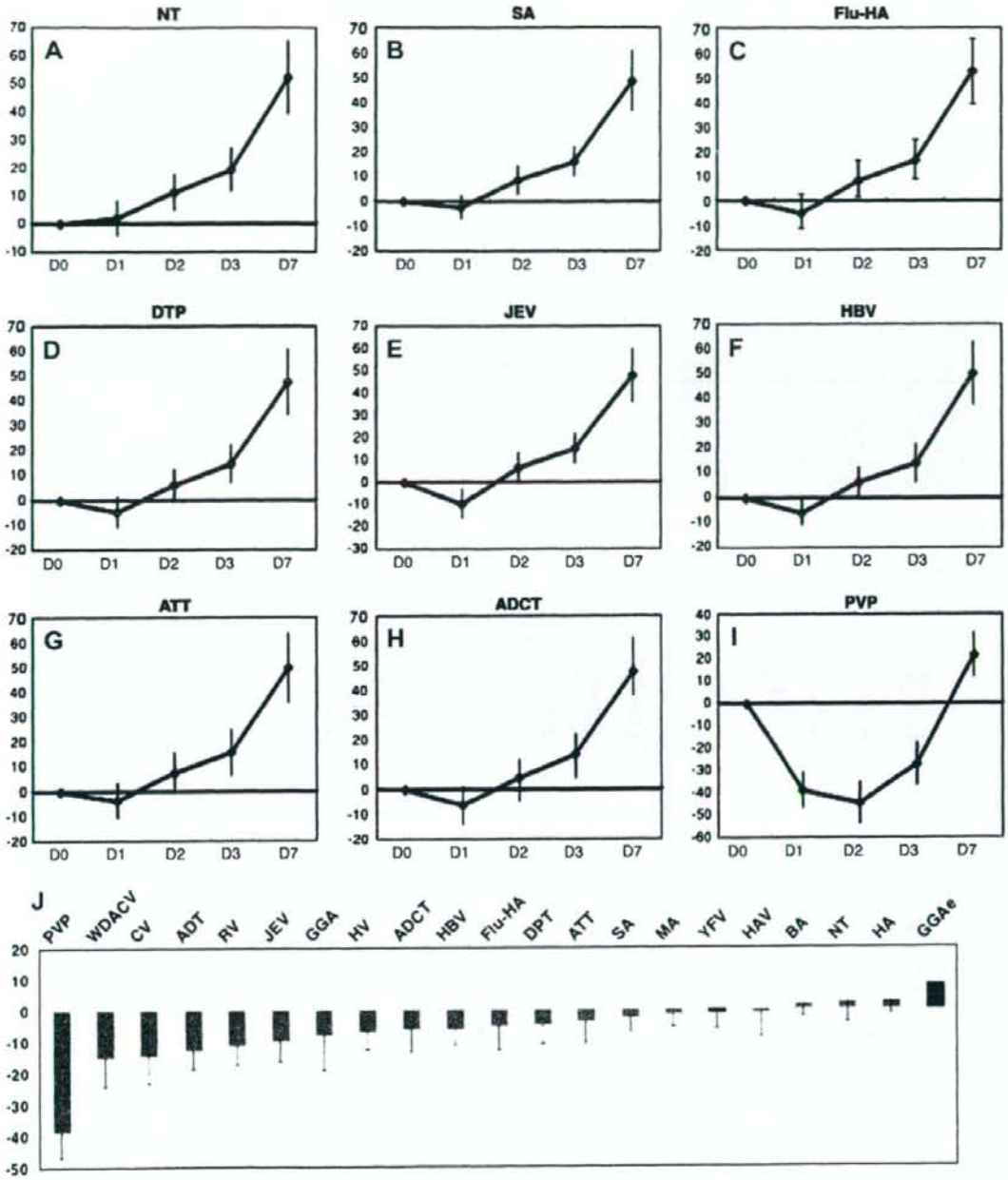

Fig. 2. Effects of several vaccine treatments on guinea pig body weight. Body weight changes after vaccination. (A) non-treated (NT) and (B) saline (SA)-treated animals as a control. (C) influenza HA vaccine (Flu-HA), (D) adsorbed diphtheria-purified pertussis-tetanus combined vaccine (DTP), (E) Japanese encephalitis vaccine (JEV), (F) hepatitis B vaccine (HBV), (G) adsorbed tetanus toxoid (TT), (H) adsorbed diphtheria-tetanus combined toxoid (ADCT), (I) pneumococcal vaccine polyvalent (PVP). (J) Body weight changes at day 1. WDACV, Weil's disease and Akiyami combined vaccine; CV, cholera vaccine; RV, rabies vaccine; GGA, freeze-dried gas gangrene antitoxin, equine; HV, adsorbed habu-venom toxoid; MA, freeze-dried mamushi antivenom, equine; HAV, freeze-dried inactivated tissue culture hepatitis A vaccine; BA, freeze-dried botulism antitoxin, equine; HA, freeze-dried habu antivenom, equine; GGAE, gas gangrene antitoxin, equine.

pathological changes were characteristic to each vaccine, and occurred not only in animals receiving the re-tested and rejected vaccines, but also in the passed vaccines, especially in the DPT, aluminum adsorbed vaccine and toxoid. The degree of pathological change varied, though no significant differences were found between controls and the test vaccines ($P < 0.05$). These data indicate that the pathological changes were due to the reactogenicity of the vaccines, rather than their

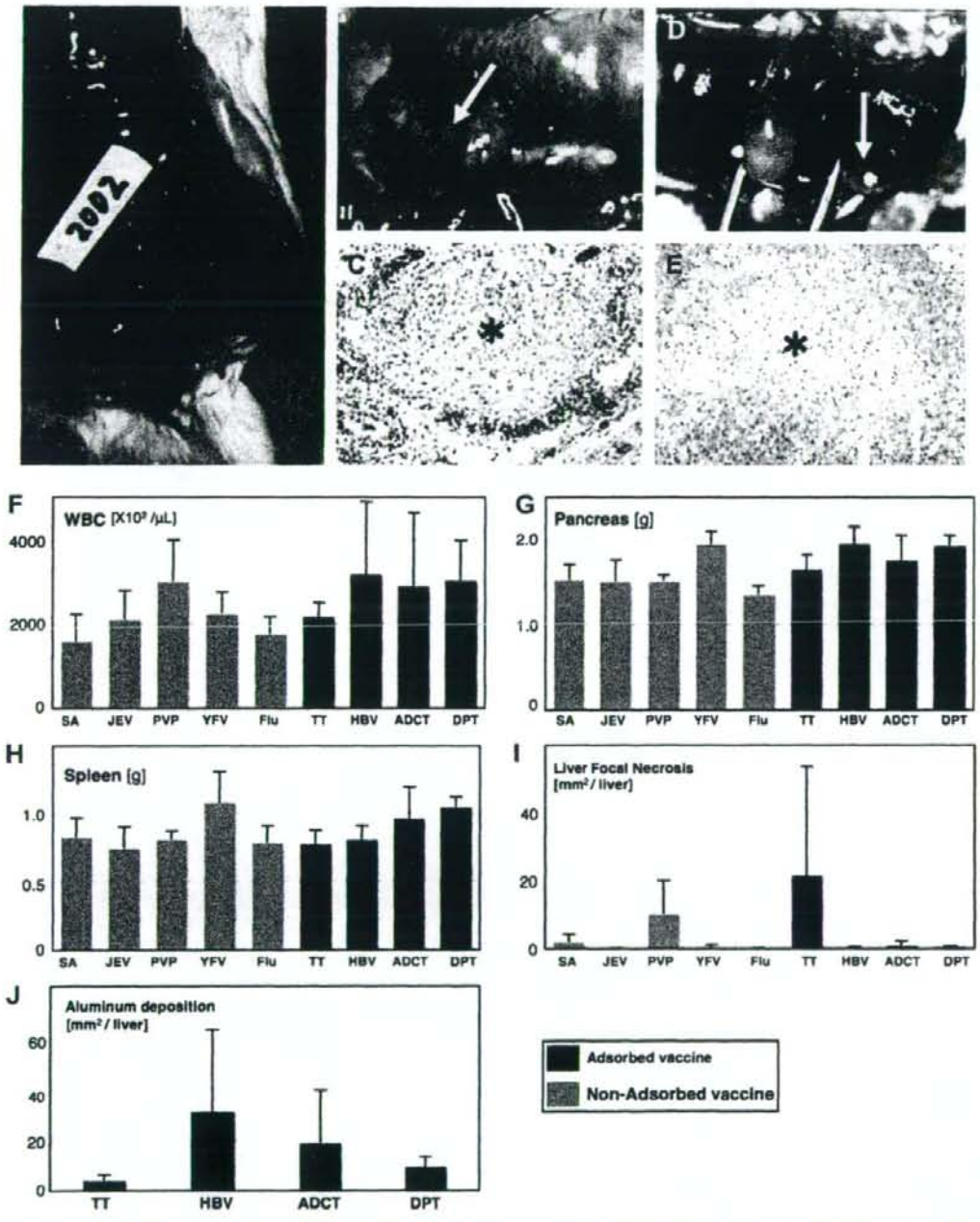

Fig. 3. Histopathological analysis in the guinea pig after vaccination. (A) Specific toxic and pathological changes, such as hemorrhagic ascites in the abdomen of the DPT-treated guinea pigs at day 7. (B) Inflammation in the DPT-treated pancreas at day 7. (C) Histological analysis of inflammation in the DPT treated pancreas by hematoxylin and eosin staining (H E). (D) Focal necrosis in the DPT-treated liver at day 7. (E) Histological analysis of focal necrosis in the DPT-treated liver. H E staining. (F) The number of leukocytes in the peripheral blood after vaccination at day 7. (G) Pancreas weight after vaccination at day 7. (H) Spleen weight after vaccination at day 7. (I) The area of focal necrosis in the vaccine-treated liver (mm^2). (J) Total area of aluminum deposition in the pancreas (mm^2). NT, non-treated; SA, saline; Flu-HA, influenza HA vaccine; DTP, adsorbed diphtheria-purified pertussis-tetanus combined vaccine; JEV, Japanese encephalitis vaccine; HBV, hepatitis B vaccine; TT, adsorbed tetanus toxoid; ADCT, adsorbed diphtheria-tetanus combined toxoid; PVP, pneumococcal vaccine polyvalent.

toxicity. These histopathological reference data will help us to define the criteria for abnormal toxicity levels in histopathological analyses.

3.4. Effects of animal grade change on ATT

To improve the quality of histopathological analyses, 'clean' animals need to be substituted by SPF animals. Our body weight RP was based on 'clean' animals, and we needed to determine the effect of changing the animal grade on the results of ATT. To validate the reliability and reproducibility of our reference population based on 'clean' animals, we focused on the vaccines (Flu-HA, DTP, YFV, JEV, HBV, TT, ADCT, PVP) for which a RP of body weights and histopathological features had already been established and confirmed in our current ATT.

Compared with the RP based on 'clean' guinea pigs, no significant differences in body weight changes were observed in NT, SA, Flu-HA, DTP, JEV, HBV, TT, ADCT and PVP-treated SPF guinea pigs ($P < 0.01$). Strong correlations between body weight changes in the 'clean' and SPF-based RPs were demonstrated (Fig. 4). Using the SPF-based RP, the conclusions from ATT based on the 'clean' RP were not changed.

3.5. Effects of animal grade change on pathological changes

To validate our modified ATT, we compared the data obtained with clean animals with those obtained with SPF animals. No significant differences in body weight changes were observed in NT, SA, Flu-HA, DPT, JEV, HBV, TT, ADCT and PVP-treated SPF guinea pig ($P < 0.01$) (Fig. 4). Pathological changes were similar for the both group injected with JEV, PVP, YFV, Flu-HA, TT, HBV, ADCT and DPT. The WBC (Fig. 5A), the pancreas (Fig. 5B) and spleen weights (Fig. 5C), and the area of focal necrosis in the liver (Fig. 5D) and area of aluminum deposition (Fig. 5E) were similar in both sets of animals ($P < 0.05$).

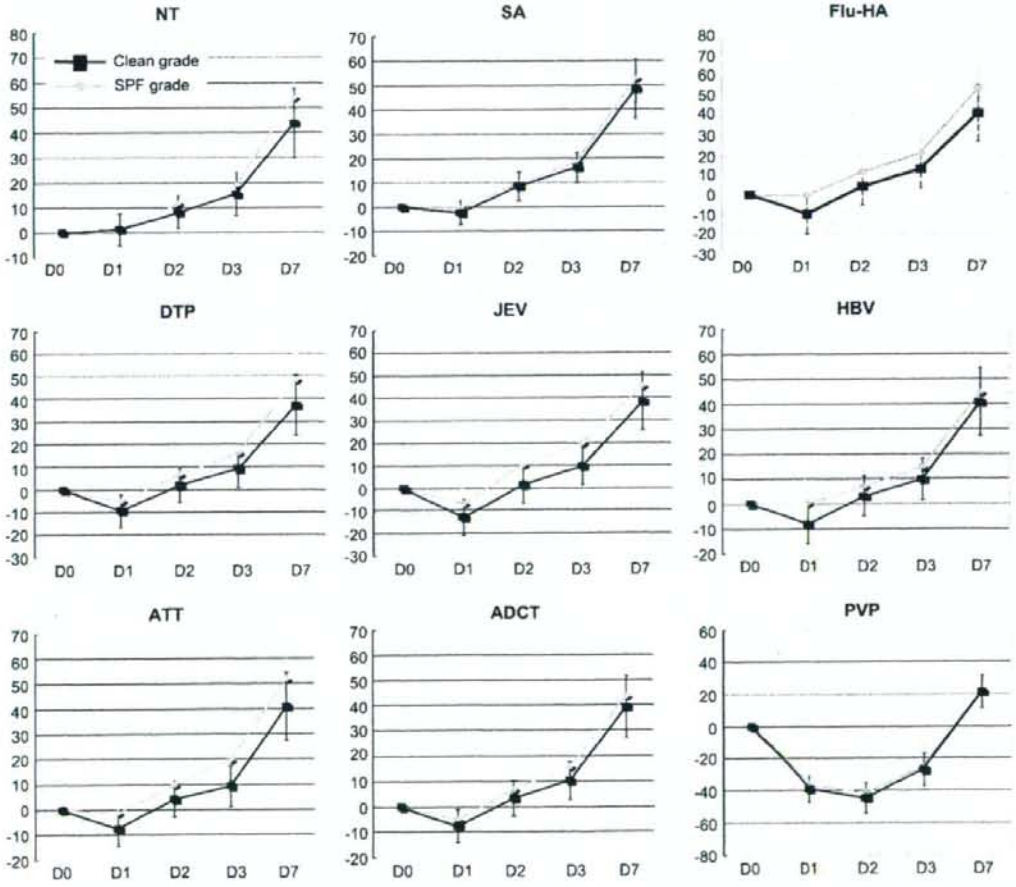

Fig. 4. Effects of animal grade changes from 'clean' to specific pathogen-free (SPF). The body weight changes after vaccination in the SPF reference group were similar to those in the 'clean' reference group. A strong correlation in body weight change was observed between the 'clean' and SPF-based reference populations. NT, non-treated; SA, saline; Flu-HA, influenza HA vaccine; DTP, adsorbed diphtheria-purified pertussis-tetanus combined vaccine; JEV, Japanese encephalitis vaccine; HBV, hepatitis B vaccine; TT, adsorbed tetanus toxoid; ADCT, adsorbed diphtheria-tetanus combined toxoid; PVP, pneumococcal vaccine polyvalent.

3.6. Proposal of improved ATT (Fig. 6)

The diagram of the improved protocol for ATT is shown in Fig. 6. It has two steps: first, arriving animals weighing 280–300 g were monitored for 7 days and only healthy animals are used for ATT. The animals are then randomly allocated to control and vaccine-treated groups, each consisting of two animals. After vaccine injection, the body weight is monitored for 7 days. If there is no significant deviation ($P < 0.01$) from RP values in Table.1, vaccines are considered to have passed the test. If a significant difference is found, histopathological analyses should be performed and the test should be repeated

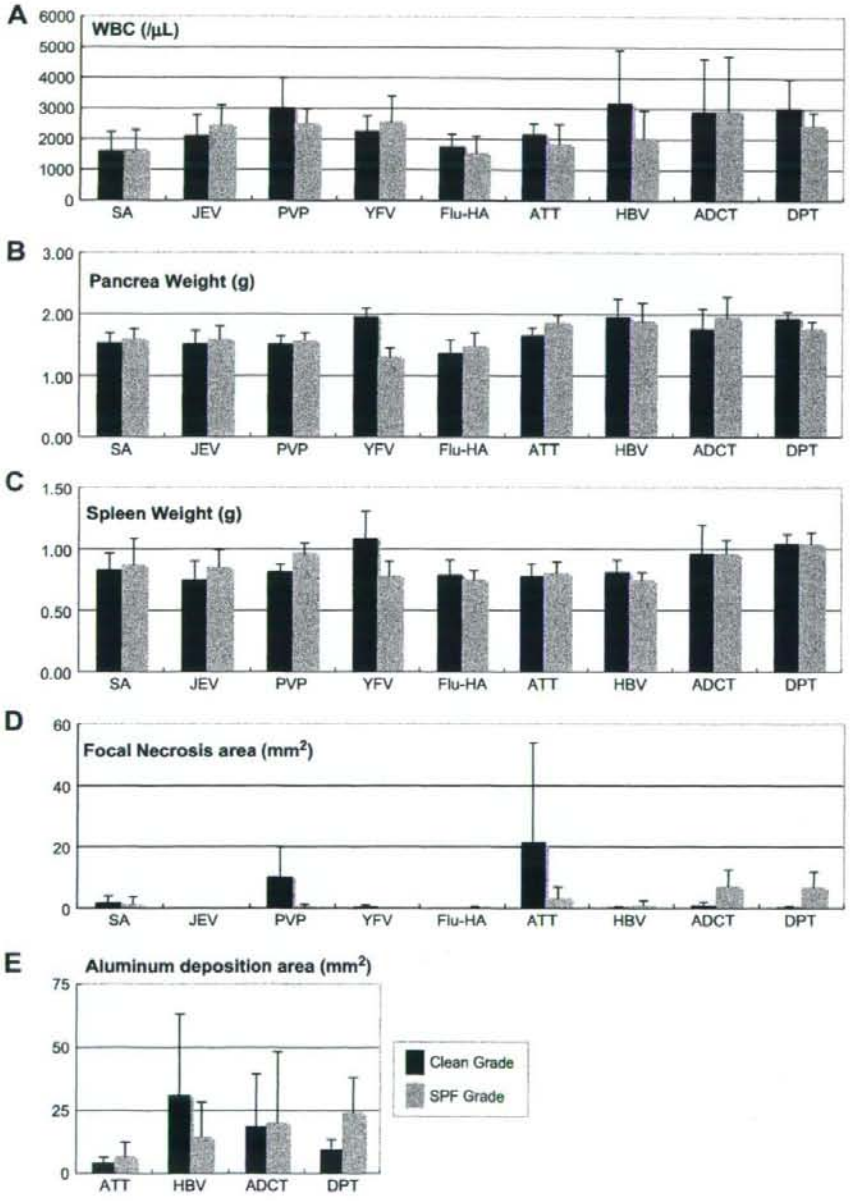

Fig. 5. Comparison of histopathological data between 'clean' and specific pathogen-free (SPF) reference groups. (A) The number of leukocytes, (B) pancreas weight, (C) spleen weight, (D) the area of focal necrosis in the liver, (E) total area of aluminum deposition in pancreas were similar in the 'clean' and SPF-based reference populations. NT, non-treated; SA, saline; Flu-HA, influenza HA vaccine; DTP, adsorbed diphtheria-purified pertussis-tetanus combined vaccine; JEV, Japanese encephalitis vaccine; HBV, hepatitis B vaccine; TT, adsorbed tetanus toxoid; ADCT, adsorbed diphtheria-tetanus combined toxoid; PVP, pneumococcal vaccine polyvalent; YFV, yellow fever vaccine.

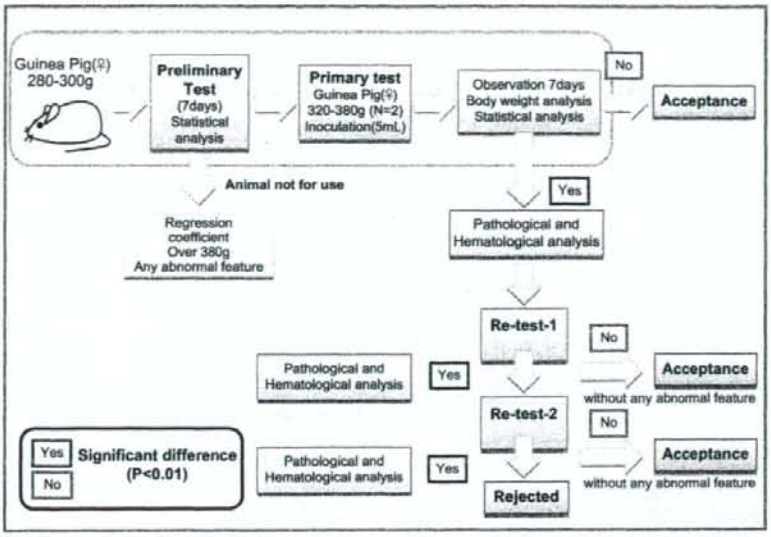

Fig. 6. Criteria of Japanese abnormal toxicity test.

at least twice. If, after two re-tests, the results are still significantly different, the vaccine is considered to have failed.

4. Discussion

ATT is performed as a safety test, in accordance with the WHO guidelines [3]. These tests ensure that the minimum requirements for vaccine safety and consistency between vaccine batches are met in Japan [4] and in other countries [5]. In Japan, tests performed by the National Regulatory Authority are important for ensuring the minimum safety requirements for vaccines. In this study, we improved the current ATT by using combined statistical and histopathological analyses and by comparing the results with RPs based on previously-passed vaccines. Since introducing these new methods to ATT, the number of re-tests has decreased and the number of animals used in ATT for DPT has been reduced from 3 to 2. Using statistical and histopathological analyses, the accuracy of the test has been improved. These test methods will enhance vaccine safety and quality control. Our method can be easily applied and is useful for vaccine manufacture by constructing a vaccine specific reference population based on the currently passed 50 lots of vaccines. Together with our data, these methods will help to understand internal quality control and future validation study for manufactures.

In the EU, in order to conform to the '3R' principle [13], animal safety tests for vaccines, sera and immunogloblins were abolished after the introduction of Good Manufacturing Practice (GMP) and Good Laboratory Practice (GLP) principles. In the US, however, the general safety test is still required by the FDA for vaccines for human use. Whether or not ATT is relevant for determining the safety of vaccines is an ongoing discussion [14]. In the US, whole blood, red blood cells, cryoprecipitated antihemophilic factor (AHF), platelets, plasma, and cellular therapy are not required to pass ATT and are described in US the Code of Federal Regulations (CFR) (21 CFR 610.118) [15]. Recently, the FDA amended the 21 CFR 610.118(g), such that manufacturers can now submit a request for exemption from ATT requirements to the director of the Center for Biologics Evaluation and Research (CBER), if they believe that their product is not appropriate for ATT, or if they can demonstrate alternative methods to ensure the safety of their products [5].

In Japan, ATT are aimed at ensuring the safety and consistency of vaccine batches. It has been suggested that adsorbed toxoid [16] and DPT [17] cause specific histopathological effects in treated animals. We proposed the aforementioned modified protocol of ATT, whose result was not affected by using the clean animal in place of SPF animals. ATT with additional statistical and histopathological analyses should therefore be the first choice for determining vaccine safety and quality.

The use of ATT for blood products was abolished in Japan in 2005, more than 10 years after the introduction of GMP regulations covering these products. This abolition resulted in an 80% reduction in animal use for ATT in Japan (data not shown). This refinement [18] in the use ATT is consistent with the spirit and concept of the '3R' principle [13].

It has been suggested that ATT cannot detect target substances causing adverse events and body weight changes. Although the mechanism causing body weight change is still unclear, Hamaguchi et al. reported that the reactogenicity and toxicity of pertussis vaccine in the rat was strongly correlated with global gene expression patterns in the liver, and they identified biomarkers relating to the pertussis vaccine-related toxicity [19]. Mizukami et al. also reported that global gene expression patterns were strongly correlated with ATT and the other current regulatory test, the leukopenic toxicity test, performed in Japan [20]. It has been suggested that reductions in body weight were due to nutritional changes caused by

changes in water consumption by animals after vaccination [21]. The two gene profiles established following pertussis vaccine and influenza vaccine treatment were different, suggesting that body weight reduction occurred as a result of changes in the expression of different genes in animals treated with different vaccines. Furthering improvements in ATT is one of the most important roles for the NRA in Japan.

In this study, we have reported on an improved method for ATT, including statistical and histopathological analyses. It based on the observation that there is body weight change characteristic to each vaccine, and such standardized changes can be used as references for evaluating test vaccines. Our improved method can both evaluate the degree of vaccine toxicity itself and lot-to-lot difference in vaccine. These improvements will help to ensure the safety and quality of vaccines.

Acknowledgements

We would like to acknowledge the contribution of the association of biological manufacturers of Japan in Tokyo. The authors are grateful to Dr Haruo Watanabe for some useful discussions and Hiroshi Yoshikura for his critical reading of our manuscript. This work was partly supported by Health and Labour Sciences Research Grants for Research on Regulatory Science of Pharmaceuticals and Medical Devices from the Ministry of Health Labour and Welfare, Japan.

References

[1] Plotkin SL, Plotkin SL. A short history of vaccination. In: Plotkin S, Orenstein W, Offit P, editors. Vaccines. 5th ed. Philadelphia, PA: WB Saunders; 2008. p. 1–16.

[2] Baylor NW, Midthun K. Regulation and testing of vaccines. In: Plotkin S, Orenstein W, Offit P, editors. Vaccines. 5th ed. Philadelphia, PA: WB Saunders; 2008. p. 1611–27.

[3] WHO Expert Committee on Biological Standardization. 30th Report. General Considerations for combined vaccine. WHO Tech Rep Ser 1979; 638:100.

[4] Minimum requirements for biological products, Japan, National Institute of Infectious Diseases, http://www.nih.go.jp/niid/MRBP/seibutsuki_english.pdf.

[5] Code of Federal Regulations. Title 21, Vol. 7, CITE: 21 CFR 610.11, http://www.accessdata.fda.gov/scripts/cdrh/cfdocs/cfcfr/CFRSearch.cfm?fr=610.11.

[6] Castle P. Alternatives to animal testing: achievements and recent developments in the European Pharmacopoeia. Dev Biol Stand 1996;86:21–9.

[7] Kurokawa M, Murata R. On the toxicity of the "toxoid" preparation responsible for the Kyoto catastrophe in 1948. Jpn J Med Sci Biol 1961; 14:249–56.

[8] Kurokawa M, Ishida S, Kuratsuka K. On the biological assay of toxicity of pertussis vaccine using mice. I. Selection of response metameter and reproducibility of relative toxicity. Jpn J Med Sci Biol 1962;15:67–84.

[9] van Zutphen LF. Toxicity testing and genetic quality control. J Exp Anim Sci 1993;35:202–9.

[10] Festing MF. A case for using inbred strains of laboratory animals in evaluating the safety of drugs. Food Cosmet Toxicol 1975;13:369–75.

[11] Cuba-Caparó A, Myers DM, Germino NI. Focal hepatic necrosis in clinically normal guinea pigs: bacteriological and pathological studies. J Comp Pathol 1977;87:441–50.

[12] Fleisher MS, Loeb L. The experimental production of necrosis of the liver in the guinea pig. J Exp Med 1914;20:169–79.

[13] Cussler K. A 4R concept for the safety testing of immunobiologicals. Dev Biol Stand 1999;101:121–6.

[14] Advisory Group on Alternatives to Animal Testing in Immunobiologicals. The target animal safety test—is it still relevant? Biologicals 2002;30:277–87.

[15] Revisions to the general safety test requirements for biological products—FDA. Direct final rule: confirmation in part and withdrawal in part. Fed Regist 1998;63:41718.

[16] Goto N, Kato H, Maeyama J, Eto K, Yoshihara S. Studies on the toxicities of aluminium hydroxide and calcium phosphate as immunological adjuvants for vaccines. Vaccine 1993;11:914–8.

[17] Goto N, Kato H. Accumulation of ascites and increase in skin vascular permeability observed by injection of adsorbed diphtheria-purified pertussis–tetanus combined vaccine in guinea pigs. Microbiol Immunol 1991;35:1143–8.

[18] Chino F. The views and policy of the Japanese control authorities on the three Rs. Dev Biol Stand 1996;86:53–62.

[19] Hamaguchi I, Imai J, Momose H, Kawamura M, Mizukami T, Kato H, et al. Two vaccine toxicity-related genes Agp and Hpx could prove useful for pertussis vaccine safety control. Vaccine 2007;25:3355–64.

[20] Mizukami T, Imai JI, Hamaguchi I, Kawamura M, Momose H, Naito S, et al. Application of DNA microarray technology to influenza A/Vietnam/1194/2004 (H5N1) vaccine safety evaluation. Vaccine 2008;26: 2270–83.

[21] Dubos R, Costello R, Schaedler RW. The influence of endotoxin administration on the nutritional requirements of mice. J Exp Med 1965; 122:1003–15.

Vaccine 26 (2008) 4686–4696

Contents lists available at ScienceDirect

Vaccine

journal homepage: www.elsevier.com/locate/vaccine

Application of quantitative gene expression analysis for pertussis vaccine safety control☆

Isao Hamaguchi[a,1], Jun-ichi Imai[b,1], Haruka Momose[a,1], Mika Kawamura[b,c], Takuo Mizukami[a], Seishiro Naito[a], Jun-ichi Maeyama[a], Atsuko Masumi[a], Madoka Kuramitsu[a], Kazuya Takizawa[a], Hiroshi Kato[a], Tetsuya Mizutani[d], Yoshinobu Horiuchi[e], Nobuo Nomura[f], Shinya Watanabe[b], Kazunari Yamaguchi[a,*]

[a] Department of Safety Research on Blood and Biological Products, National Institute of Infectious Diseases, 4-7-1 Gakuen, Musashimurayama, Tokyo 208-0011, Japan
[b] Department of Clinical Informatics, Tokyo Medical and Dental University, Tokyo, Japan
[c] Medicrome, Inc., Sendagaya, Shibuya-ku, Tokyo 151-0051, Japan
[d] Department of Virology I, National Institute of Infectious Diseases, 4-7-1 Gakuen, Musashimurayama, Tokyo 208-0011, Japan
[e] Department of Bacterial Pathogenesis and Infection Control, National Institute of Infectious Diseases, 4-7-1 Gakuen, Musashimurayama, Tokyo 208-0011, Japan
[f] Biological Information Research Center, National Institute of Advanced Industrial Science and Technology, Japan

ARTICLE INFO

Article history:
Received 19 February 2008
Received in revised form 10 June 2008
Accepted 15 June 2008
Available online 9 July 2008

Keywords:
Pertussis vaccine
Microarray
Safety test
Quantitative analysis

ABSTRACT

Although vaccines are routinely used to prevent infectious diseases, little is known about the comprehensive influences caused by vaccines. In this study, we showed, using comprehensive gene expression analysis, that pertussis vaccine affected many genes in multiple organs of vaccine-treated animals. In particular, lung was revealed to be the most suitable target to evaluate pertussis vaccine toxicity. The 13 genes identified from the analysis of vaccine-treated lung at day 1 showed a clear dendrogram corresponding to pertussis vaccine toxicity. Furthermore, quantitative analysis of these genes revealed a positive correlation between their respective expression levels and the degree of toxic effects observed in samples that had been treated with various doses of reference pertussis vaccines. The quantification of this 13 gene-set is an indicator of the vaccine toxicity-related reaction.

1. Introduction

Vaccination is among the most significant public health success stories of all time. However, like any pharmaceutical product, no vaccine is completely safe. While a large part of known vaccine adverse events is minor and self-limited, some vaccines have been associated with very rare but serious health effects. Whole-cell pertussis vaccine is composed of a suspension of inactivated *Bordetella pertussis* cells, whereas acellular pertussis vaccines contain purified, inactivated components of *B. pertussis* cells. Current acellular pertussis vaccines mostly contain pertussis toxin (PT) and filamentous hemagglutinin [1]. As with all injected vaccines, administration of pertussis vaccine may cause local reactions, such as pain, redness, or swelling in 20–40% of treated children [2]. Moderate or severe systemic events, such as fever 105 °F or higher, febrile seizures and hypotonic–hyporesponsive episodes, have been reported [2]. Until now the adverse reaction of the vaccine has not been fully elucidated.

So far, fundamental to preventing safety problems with vaccines is the assurance that any vaccines for public use are made using Good Manufacturing Practices (GMP) with prerelease lot-testing for purity and potency. Furthermore, manufacturers must submit samples of each vaccine lot and results of their in-house tests for potency and purity to national control authorities before releasing them into clinical use. Conventional animal toxicity tests have been performed to detect the general toxicity of vaccines because the remaining toxicity of vaccines has the potential to cause adverse reactions. For example, the animal body weight decreasing test is the most commonly used control test to evaluate the toxicity of vaccines [3]. The body weight loss of vaccine-treated mice should be less than 10% of the whole weight for the regulation of safety of the vaccine. Although a correlation of the results from the body weight decreasing test with the vaccine's toxicity has been shown [4], a greater understanding of the molecular mechanisms involved in the development of vaccine toxicity needs to be clarified.

☆ This work was supported by Grants-in-Aid from the Ministry of Health, Labour and Welfare, Japan.

* Corresponding author.
E-mail address: kyama@nih.go.jp (K. Yamaguchi).

[1] These authors contributed equally to this work.

0264-410X/$ – see front matter © 2008 Elsevier Ltd. All rights reserved.
doi:10.1016/j.vaccine.2008.06.086

Table 1
Sequence of primers used in this study

Symbol	Primer concentration	Forward primer sequence	Reverse primer sequence
S100A8	200 nM	5′-TGCCCTCAGTTTGTGCAGAATA-3′	5′-CCAACGCAAGGAACTCTTCGA-3′
S100A9	200 nM	5′-GACCACAGGCACGGCAAAG-3′	5′-CCCAGCCCCAGAACCAAG-3′
CCL2	200 nM	5′-TTTCCACAACCACCTCAAGCA-3′	5′-TAAGGCATCACATTCCAAATCACA-3′
MMP8	200 nM	5′-AACAACCAATGCTGGAGATACGAC-3′	5′-GCATCAATTCTACAGTTTATTCCTGGG-3′
MCPT9	100 nM	5′-GTGCCAAGGCATGTCCAGAA-3′	5′-CCAGCAGTAGCCTTCCTCTCATT-3′
MMP9	50 nM	5′-AGGTGGATCCCCAGAGCGT-3′	5′-TTGGTAGTGAAAGACGTTGTGTGAG-3′
BEST5	200 nM	5′-TGTGCATGTATCTCCCTGTAGAATGA-3′	5′-TTTAATACACAGATCACGTTTCCATACACT-3′
MX2	200 nM	5′-AAGGAACATAGTGACACCAGTGAGAAG-3′	5′-GGACAGGGCCAGCTTAACCA-3′
IRF7	100 nM	5′-TGCAGCGTGAGGGTGTGTC-3′	5′-TCATCGTAGAGACTATTGGTGCTAGACA-3′
IFI27L	50 nM	5′-AAGGTCCTCGTGGGCTCTACAG-3′	5′-TTATCAGAGGAAGGAGTACAAATGCTTAC-3′
IFIT3	100 nM	5′-CCCTGAAGGATCTCATGCAGTTT-3′	5′-TCCGTTCTGCGTTTGCTGTT-3′
CYP2E1	200 nM	5′-GAAAGCGTGTGTGTGTTGGAGA-3′	5′-AACTGTGACAGGACTGAGGTCGAT-3′
NGP_predicted	100 nM	5′-GTTAATCGGGCCATAGAGGCATA-3′	5′-CAGGAGGTGGAGTGGCACTTAG-3′
GAPDH	200 nM	5′-GTGAAGCTCATTTCCTGGTATGACA-3′	5′-TTCTTACTCCTTGGAGGCCATGTAG-3′

Gene expression profiling is a unique way to characterize how cells are affected by alterations in pathologic conditions. The measurements of gene expression levels upon exposure to toxicants can be used both to provide information about the mechanism of action of the toxicant and to form a "genetic signature" for the identification of toxic products. The development of high-quality gene arrays has allowed this technology to become a standard tool in molecular toxicology. Recently, the field of toxicogenomics has validated the concept of gene expression profiles as "signatures" of toxicant classes. These signatures have effectively directed the analytical search for predictive biomarkers of toxicant effects and contributed to the understanding of the dynamic alterations in molecular mechanisms that are associated with toxic responses.

Many studies of gene expression profiles have been reported in the toxicology field. For example, Hamadeh et al. reported the patterns of gene expression in liver tissue taken from rats exposed to different chemicals [5]. Moreover, DNA microarray assays have been applied as an evaluation method for analyzing side effects of medicines [6].

Although DNA microarray analysis was used to detect the toxicity of pharmaceuticals as shown above, vaccine-related genes have not been evaluated using comprehensive gene expression analysis. The principle of nucleic acid hybridization is not new, however, microarrays have opened the way for the parallel detection and analysis of expression patterns of thousands of genes in a single experiment. Moreover, the sensitivity of microarrays allows for the detection of subtle differences that are much harder to detect with subtraction or other molecular methods. For a better understanding of the molecular toxicology regarding vaccines, the DNA microarrays are ideal methods.

In this study, we tried to identify the "genetic signatures" for the toxicants in the pertussis vaccine using DNA microarray analysis, and subsequently developed a gene expression detection system for pertussis vaccine toxicity.

2. Materials and methods

2.1. Animals

8-week-old male Wistar rats weighing 160–200 g were obtained from SLC (Tokyo, Japan). All animals were housed in rooms maintained at 23 ± 1 °C, with 50 ± 10% relative humidity, and 12-h light/dark cycles for at least 1 week prior to the test challenge.

2.2. Vaccines and toxin

Reference pertussis vaccine (reference vaccine; RE) is a lyophilized whole cell preparation of pertussis organisms treated for inactivation with formaldehyde, and has been used for National Quality Control Tests on pertussis vaccine in Japan since 1981. It was reconstituted in 12 ml of physiological saline, and 5 ml was injected intra-peritoneally (IP). From the conventional leukocyte promoting test, RE is predicted to contain the pertussis toxin at the concentration of 5 μg/ml. PV is a purified pertussis vaccine (a generous gift of The Chemo-Sero-Therapeutic Research Institute, Kumamoto, Japan) and contains inactivated pertussis toxin. Pertussis toxin (PT) (Wako chemicals, Osaka, Japan) and PV were adjusted to 5 μg/ml (PT concentration). RE, PV, and PT were injected into rats IP (5 ml/rat). Five milliliters of saline (SA) were injected as a control.

2.3. Body weight decreasing test

The rat body weight decreasing test was performed according to the Minimum Requirements of Biological Products [7]. We injected 5 ml of samples into the rat peritoneum for the treatment and rat weight was measured for 1 week after injection.

2.4. RNA preparation

Rats were sacrificed to obtain the whole lung, kidney, brain, and the lateral left lobe of the liver. Organs were immediately frozen in liquid nitrogen for storage. Thawed tissue was homogenized and

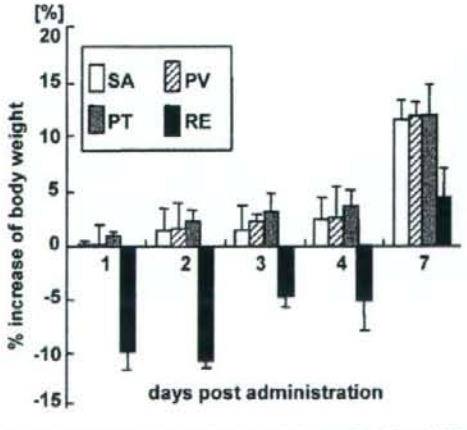

Fig. 1. Biological analysis of the vaccine-treated animals. The effects of RE, PT, PV, SA-treatment were measured using rat body weight decreasing toxicity tests. All animals were weighed at days 0, 1, 2, 3, 4 and 7. Changes in rat body weight were assessed at the percentage increase or decrease, and are indicated by the mean change ± S.D. of three independent experiments.

mixed with an ISOGEN reagent (NIPPON GENE, Tokyo, Japan). Total RNA was prepared from the lysate in accordance with the manufacturer's instructions. Poly(A)+ RNA was prepared from total RNA with a Poly(A) Purist Kit (Ambion, Austin, TX), according to the manufacturer's instructions.

2.5. Microarray preparation and expression profile acquisition

For the microarray analysis, three rats per group were treated with RE, PT, PV, and SA, and four organs from each group were analyzed on day 1–4 post-treatment. In total, 48 samples from each organ were analyzed for this experiment. A set of synthetic polynucleotides (80-mers) representing 11,468 rat transcripts and including most of the RefSeq genes deposited in the NCBI database (MicroDiagnostic, Tokyo, Japan) was arrayed on aminosilane-coated glass slides (Type I; Matsunami, Kishiwada, Japan) with a custom-made arrayer [8,9]. Poly(A)+ RNA (1.5 μg) was labeled with SuperScript II (Invitrogen, Carlsbad, CA) and Cyanine 5-dUTP for each sample or Cyanine 3-dUTP (PerkinElmer, Boston, MA) for a rat common reference RNA (MicroDiagnostic). Labeling, hybridization, and washes of microarrays were performed with a Labeling & Hybridization Kit (MicroDiagnostic) according to the manufacturer's instructions. The rat common reference RNA was purchased as a single batch and labeled as an aliquot with Cyanine-3 for a single microarray side by side with each sample labeled with Cyanine-5. Hybridization signals were measured using a GenePix 4000A scanner (Axon Instruments, Whipple Road Union City, CA) and then processed into primary expression ratios ([Cyanine 5-intensity obtained from each sample]/[Cyanine 3-intensity obtained from common reference RNA], which are indicated as 'median of ratios' in GenePix Pro 3.0 software (Axon Instruments)). Normalization was performed for the median of ratios (primary expression ratios) by multiplying normalization factors calculated for each feature on a microarray by the GenePix Pro 3.0 software.

2.6. Data analysis

Data processing and hierarchical cluster analysis were performed using Excel (Microsoft, Redmond, WA) and a MDI gene expression analysis software package (MicroDiagnostic). The primary expression ratios were converted into $\log_2$ values ($\log_2$ Cyanine-5 intensity/Cyanine-3 intensity) (designated log ratios) and compiled into a matrix (designated primary data matrix). To predict the most obvious differences obtained from cluster analysis of the primary data matrix, we extracted genes with $\log_2$ ratios over 1 or under −1 in at least one sample from the primary data matrix and subjected them to two-dimensional hierarchical cluster analysis for samples and genes. To identify genes demonstrating significant changes in expression, we extracted genes by *t*-test between SA and PT-treated samples ($p < 0.01$). Among the extracted genes, we further selected genes that exhibited differences greater than 0.75 between mean averages of log ratios for the two sample groups (SA and PT).

2.7. Histology

Vaccine-treated lungs were harvested from rats and fixed in Bouin's Solution (SIGMA, St. Louis, MO) and 4% (w/v) paraformaldehyde at 4 °C for 48 h. After fixation, tissues were dehydrated through a series of graded alcohols and xylene and embedded in paraffin. Chilled paraffin blocks were cut into 4–6 μm sections, which were floated onto glass slides, dried overnight, and stained with hematoxylin and eosin (HE). Three rats per group, treated with RE, PT, PV, and SA, were analyzed on day 1 post-treatment.

Table 2
Pertussis vaccine toxicity related genes in lung

day 1	day 2	day 3	day 4
NM_053587	L18948	NM_053587	NM_053587
L18948	NM_053587	L18948	L18948
X68312	NM_022221	NM_022221	NM_022221
NM_019323	NM_022177	M57441	NM_012580
NM_053822	AF209976	NM_031530	XM_222255
M21782	NM_022524	XM_221486	NM_019296
M15402	NM_017227	XM_216379	XM_222462
NM_031055	NM_031766	NM_013154	XM_224300
Y07704	AF017638	AF062038	M15402
NM_017028	NM_012620	NM_019153	L19998
XM_215121	AF035951	NM_053822	U24441
NM_130743	XM_221486	NM_019323	NM_031315
M57441	Y07704	NM_031055	Y07704
NM_031530	XM_215208	J02585	NM_053373
X55180	XM_222462	NM_017055	NM_017183
XM_221061	NM_019296		NM_017061
AF313411	U24441		M57441
XM_220059	NM_017028		NM_031530
XM_234508	XM_215121		AB015877
NM_053769	X52711		XM_216379
NM_022221	NM_153733		XM_235354
NM_031619	NM_139186		XM_218820
D50568	NM_053373		NM_139257
J02627	NM_017061		NM_019214
XM_236646	NM_013154		NM_012620
	L31883		AF015953
	M57441		X55180
	XM_216379		XM_215121
	NM_022604		NM_017028
	L40364		X52711
	NM_031612		U02553
	NM_053687		NM_053769
	NM_019153		NM_022266
	NM_019323		NM_012862
	NM_053822		AF062038
	XM_236646		NM_031512
	NM_053929		NM_013154
	Z78279		X63369
	D50568		NM_017260
	J02627		J04035
	NM_012880		NM_019153
	J02585		AI104238
			U06436
			NM_022604
			NM_057103
			NM_053687
			NM_053822
			NM_019323
			XM_236646
			J02585
			NM_031348
			J02627
			NM_017134
			NM_012582

Gene expression patterns in SA- and PT- treated lungs were examined by microarray analysis. From the filtration with the expression ratios over 0.75 in $\log_2$ scales on average ($P < 0.01$), 25, 42, 15 and 54 genes were extracted on day 1, 2, 3 and 4, respectively.

2.8. Quantitative RT-PCR analysis

Poly(A)+ RNA was used to synthesize first-strand cDNA using a First-strand cDNA Synthesis Kit (Life Science, Inc., St. Petersburg, FL), according to the manufacturer's instructions. Expression levels of toxicity-related genes were analyzed by Real-Time PCR using a 7500 Fast Real-Time PCR System (Applied Biosystems, Foster City, CA) with 7500 Fast System SDS Software Version 1.3. cDNA was amplified for Real-Time PCR using SYBR Green I (Molecular Probes, Inc.) to detect the PCR products. One microliter of 6-fold diluted cDNA was used in a 20-μl final volume reaction containing 10 μl SYBR Green® PCR Master Mix (Applied Biosystems), and forward and reverse primers. The 7500 Fast System was programmed to run an initial polymerase activation step at 95 °C for 10 min followed by 40 cycles of denaturation (95 °C for 15 s) and extension (60 °C for 1 min). Product synthesis was monitored at the end of the extension step of each cycle. The primers for each gene were shown in Table 1. Gene expression values were normalized against rat *GAPDH*.

2.9. QuantiGene Plex assays

The QuantiGene Plex assays were performed according to the procedure of QuantiGene Plex Reagent System (Panomics), which is described in more detail elsewhere [10]. Briefly, 10 μl of starting poly(A)+ RNA (50 ng) was incubated for 10 min at 65 °C, then mixed with 33.3 μl of Lysis Mixture, 40 μl of Capture Buffer, 2 μl of Capture Beads, and 2 μl of the target gene-specific probe set. For the lung homogenate, 40 μl of lung lysates were mixed with 33.3 μl of Lysis Mixture, 0.2 μl of Proteinase K, 2 μl of Capture Beads, and 2 μl of the target gene-specific probe set. Probe sets were heated for 5 min prior to use. Each sample mixture was then dispensed into an individual well of a Capture Plate. The Capture Plate was sealed with foil tape and incubated at 54 °C for 16–20 h. The hybridization mixture was transferred to filter plate, and the wells were washed three times with 200 μl of wash buffer. Signals for the bound target mRNA were developed by sequential hybridization with branched DNA (bDNA) amplifier, and biotin-conjugated label probe, at 48 °C for 1 h each. Two washes with wash buffer were used to remove unbound material after each hybridization step. Streptavidin-conjugated phycoerythrin (SAPE) was added to the wells and incubated at room temperature for 30 min. The luminescence of each well was measured using a Luminex 100 microtiter plate luminometer (Luminex). Two replicate assays measuring RNA directly (independent sampling $n = 6$ for mRNA, $n = 3$ or 5 for lysate) were performed for all described experiments. The 13 targeted genes and *GAPDH* mRNA were quantified, and the ratio of the target genes to *GAPDH* mRNA was calculated.

3. Results

3.1. Vaccine-treated animals showed severe weight loss

In order to screen the general toxicity of vaccine, we analyzed the body weight of vaccine treated-animals. For this analysis, 5 ml of the vaccine was injected into the peritoneum of rats, and the weight loss of the treated animals was analyzed for 7 days. As shown in Fig. 1, the reference whole-cell vaccine (RE)-treated rats experienced severe decreases in body weight. The RE-treated rats lost

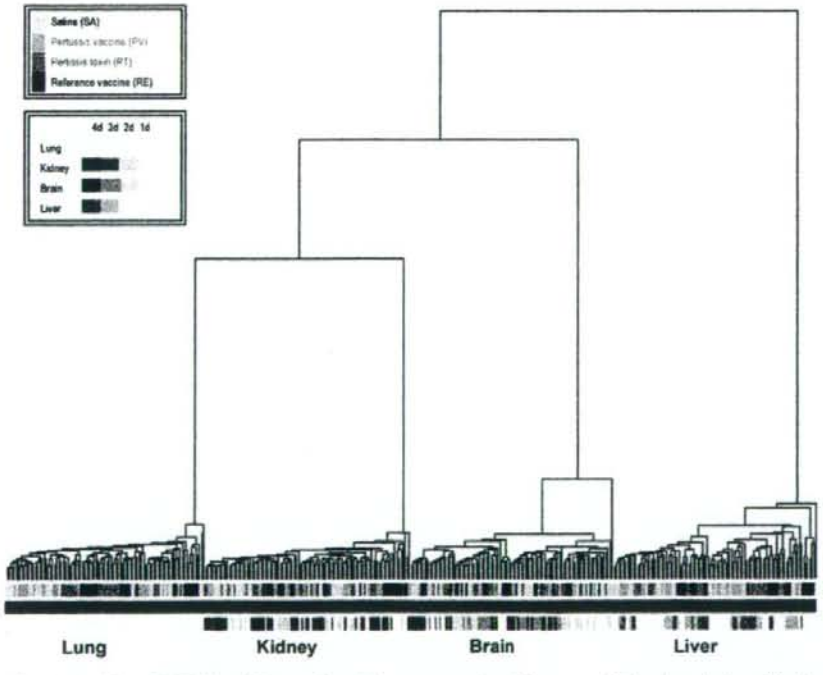

Fig. 2. Gene expression profiles obtained from RE, PT, PV and SA-treated rats. The gene expression of four organs (kidney, lung, brain and liver) was assembled in the order obtained from the results of the two-dimensional hierarchical clustering analysis. The dendrogram indicates the relationship between the samples after clustering analysis; the *y*-axis of the dendrogram depicts Euclid square distance as the dissimilarity coefficient. Color bars in pale blue, blue, green, and violet represent SA, PV, PT and RE, respectively. Blue and red bars show two independent gene profiling experiments for Exp. 1 and Exp. 2, respectively. Color bars in yellow, blue, red, and green represent lung, kidney, brain, and liver, respectively.

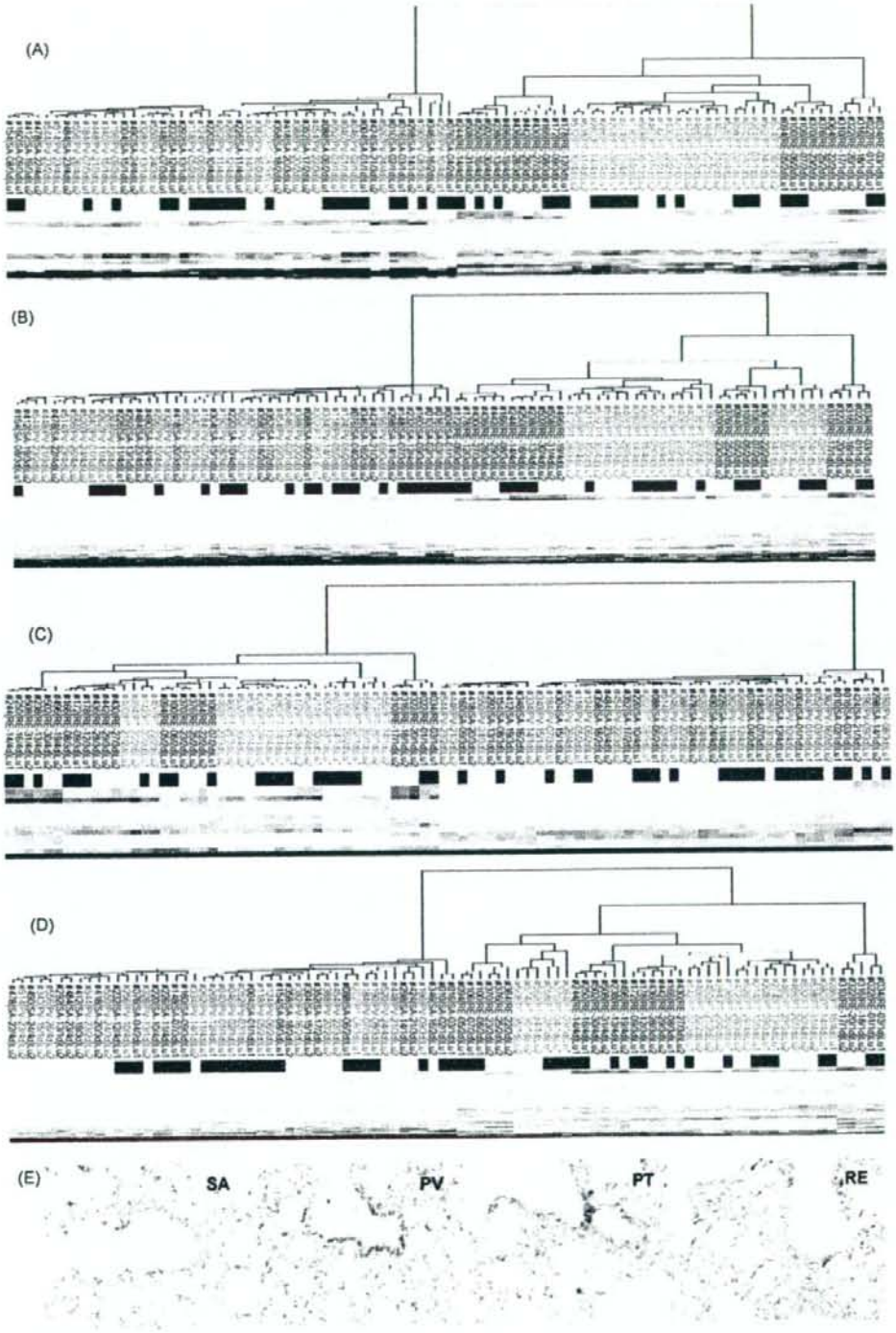

Fig. 3. Gene profiling analysis by the contrast genes between PT- and SA-treated-lungs. Specific genes, which showed large alterations between PT and SA selected by the SN method (see Section 2) included 25, 42, 15 and 54 genes at day 1 (A), day 2 (B), day 3 (C) and day 4 (D), respectively. These genes are assembled in the order obtained from the results of the two-dimensional hierarchical clustering analysis. The dendrogram for each day indicates the relationship between the samples (RE; red, PT; green, PV; blue, SA; black). Blue and yellow bars show two independent gene profiling experiments for Exp. 1 and Exp. 2, respectively. (E) The left lobes of RE, PT, PV and SA-treated lungs at day1 were stained with HE.

10% of the body weight within 1 day. Two days after treatment, the RE-treated rats started gaining weight, but it was still reduced at day 4 versus saline (SA)-treated rats. In contrast, the acellular pertussis vaccine (PV)-treated and pertussis toxin (PT)-treated rats demonstrated normal weight gain during the testing period similar to SA-treated rats.

3.2. Microarray analysis of the organ from vaccine-treated rats

To evaluate the effect of pertussis vaccine on gene expression, we prepared three rats per group in one experiment. RE-, PT-, PV-, and SA-treated animals were sacrificed to obtain the liver, lung, brain and kidney on days 1, 2, 3 and 4 post-administration. The animal experiments were performed twice with an interval of several weeks between the two experiments (designated as Exp. 1 and Exp. 2). Eventually, we obtained 96 independent tissue samples for the four time points. We labeled poly(A)+ RNA purified from the samples and a rat common reference RNA with Cyanine-5 and Cyanine-3, respectively, and hybridized to microarrays representing 11,468 transcripts. Hybridization signals were processed into expression ratios as $\log_2$ values (designated log ratios) and compiled into a matrix designated as the primary data matrix (see Section 2).

To predict the most obvious differences obtained from the clustering analysis of the primary data matrix, we extracted genes with log ratios over 1 or under −1 in at least one sample from the primary data matrix and subjected them to two-dimensional hierarchical clustering analysis for samples and genes. When the clustering

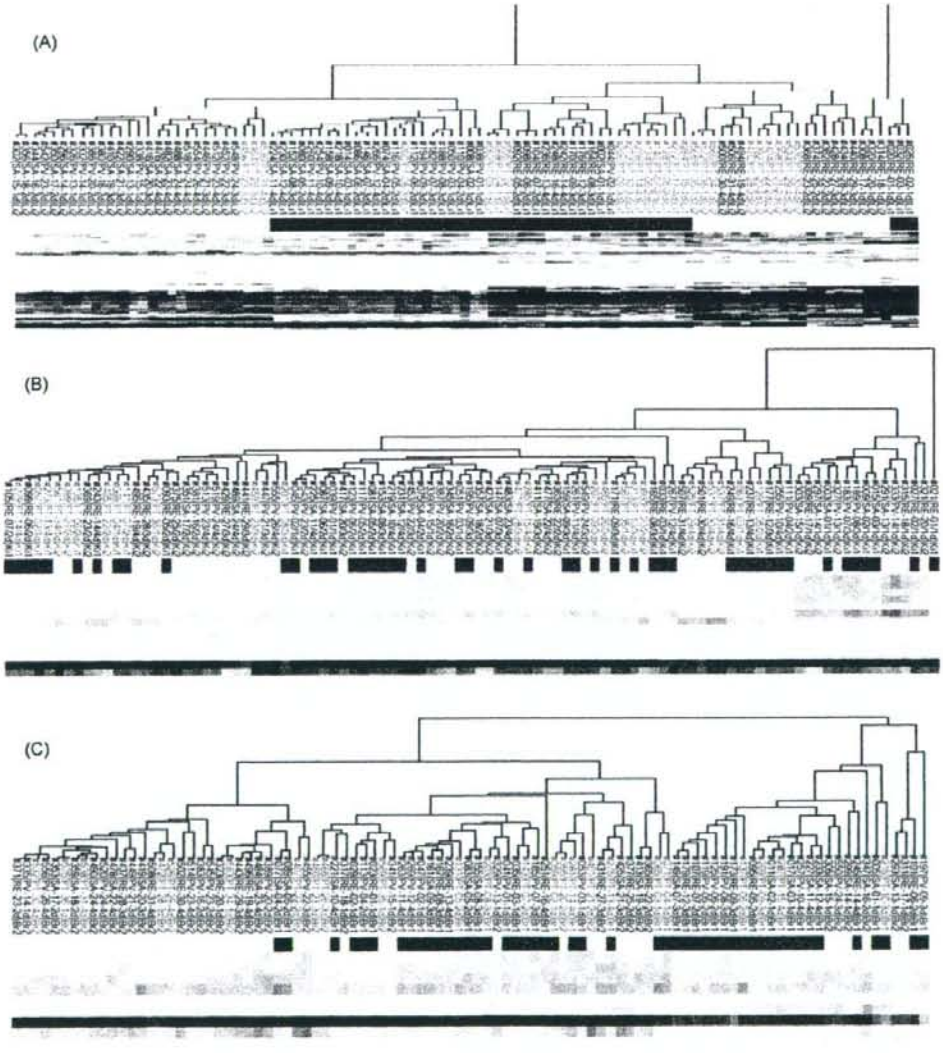

Fig. 4. Gene profiling analysis by the contrast genes between PT- and SA-treated-organs at day 1. Specific genes, which showed large alterations between PT and SA selected by the SN method (see Section 2) included 67, 14 and 9 genes from liver (A), kidney (B), and brain (C), respectively. These genes are assembled in the order obtained from the results of the two-dimensional hierarchical clustering analysis. The dendrogram indicates the relationship between the samples (RE; red, PT; green, PV; blue, SA; black). Blue and yellow bars show two independent gene profiling experiments for Exp. 1 and Exp. 2, respectively.

analysis for all samples was performed, the greatest four clusters corresponding to the individual organs were obtained as predicted. The dendrogram representing the liver, brain, lung and kidney comprised only smaller clusters (Fig. 2). The results obtained from this analysis indicate that the proceeding method of the microarray analysis is proper and by precipitating the toxicity-specific genes with statistical methods, a much sharper dendrogram will be expected.

3.3. *Vaccine-treated lung had a clear dendrogram with vaccine toxicity-related genes*

To analyze the effect of the pertussis vaccine and pertussis toxin, cluster analysis was performed with individual organs. We examined the gene expression patterns in SA- and PT-treated lungs. From the filtration with the expression ratios over 0.75 in $\log_2$ scale on average and the *t*-test ($P<0.01$) between SA and PT-treated samples, 25, 42, 15 and 54 genes were extracted on day 1, 2, 3 and 4, respectively (Table 2). Based on these genes, the clustering analysis showed two big clusters for each day, that is, RE- and PT-treated samples established a cluster that is clearly distinct from the SA- and PV-treated samples (Fig. 3). Only one sample that was treated by PT (#202 in Fig. 3) demonstrated discordance, because of a technical mistake at the administration of the toxin. We also examined the other three organs, liver, kidney, and brain. Data from SA- and PT-treated samples were compared and filtered with the expression ratios over 0.75 in $\log_2$ scale on average and the *t*-test ($P<0.01$) between SA and PT-treated samples. We extracted the marker genes on each day, and data from liver samples were reanalyzed with these genes (Fig. 4A). Unexpectedly, the resultant clusters did not necessarily correspond to the treated samples. When the expression patterns of kidney and brain were analyzed with the same procedure, the dendrograms of kidney and brain were confused as shown in Fig. 4(B and C), respectively. From these results, only the

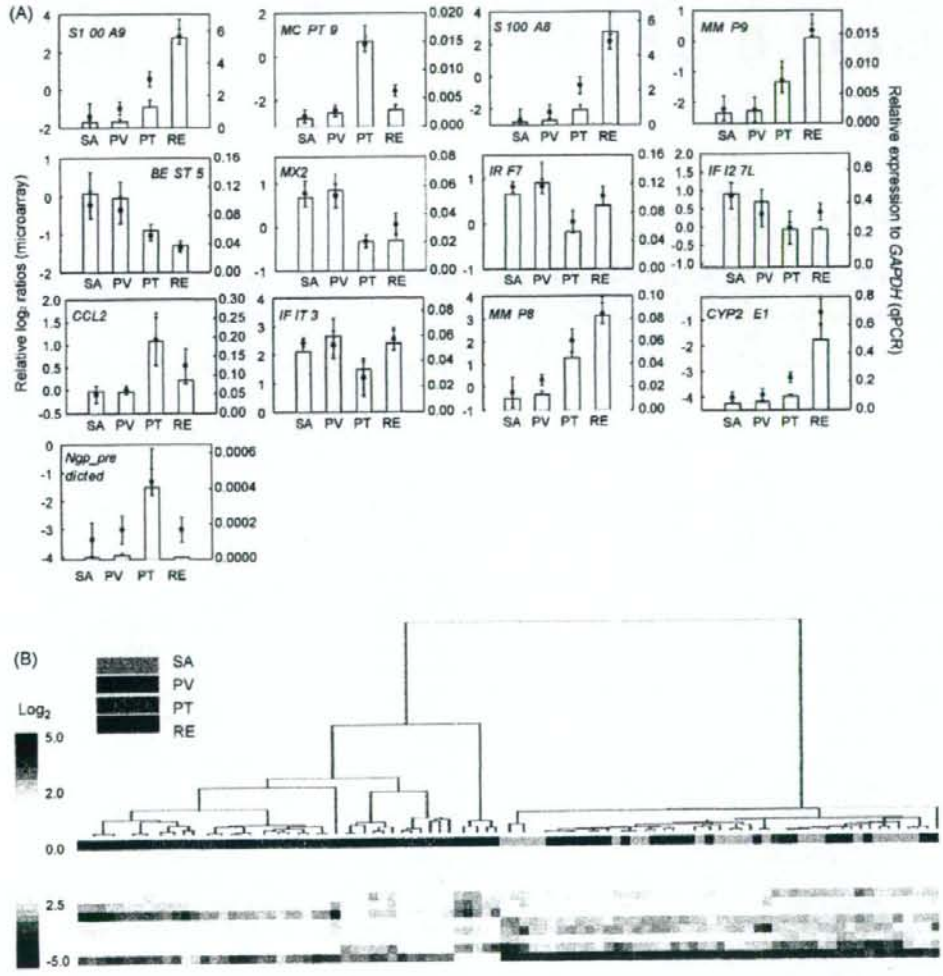

Fig. 5. Extraction of candidate genes for detection of the pertussis vaccine toxicity. (A) Expression of 13 genes from DNA microarray analysis was compared with Real-Time PCR data. Relative $\log_2$ ratios were extracted from the secondary data matrix for the 13 genes. Each symbol represents data from microarray analysis. The data of six animals in two independent experiments are shown. Expression values are indicated by the mean ratio ± S.D. Real-Time PCR analysis of the treated lung from individual animals is shown in bar graph. The data from six animals in two independent experiments are shown as the mean expression ± S.D. Quantitative PCR data was assessed relative to rat *GAPDH*. (B) Cluster analysis of day 1 samples with the selected 13 genes demonstrated a similar dendrogram to the 25 genes identified by microarray.

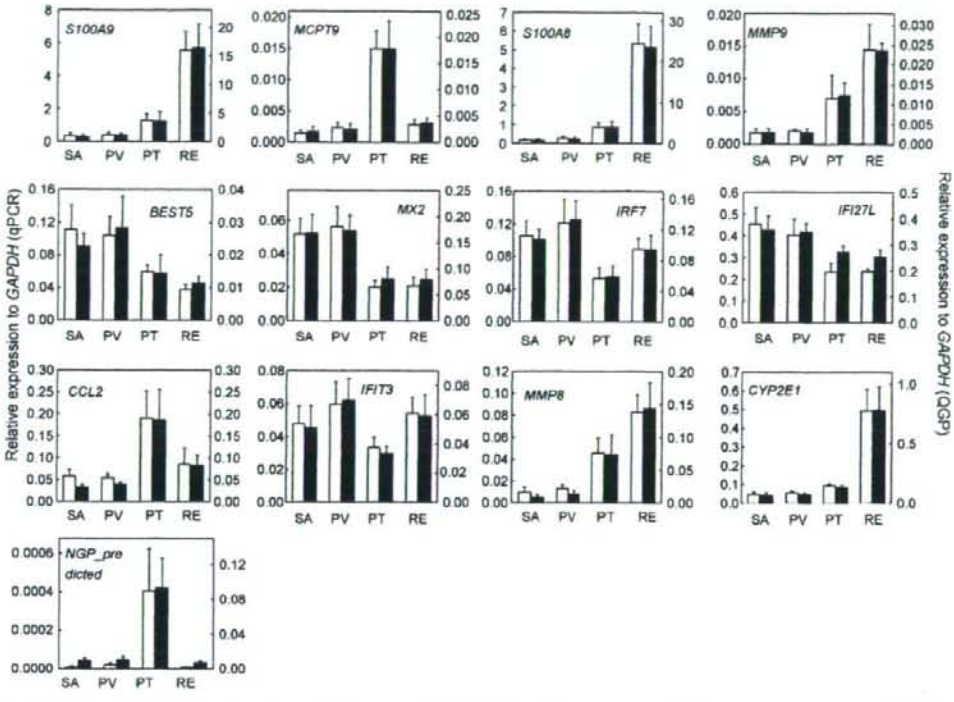

Fig. 6. Quantitative evaluation of toxicity-related genes by QuantiGene Plex. Quantification data of 13 genes with QuantiGene Plex by using poly(A)+ RNA (black bar) are compared with that of Real-Time PCR analysis (gray bar). The data from six animals in two independent experiments are shown as the mean expression ± S.D. Both Real-Time PCR data and QuantiGene Plex data were assessed relative to rat *GAPDH*.

lung is adequate to examine using gene expression-based cluster analyses.

3.4. Histological analysis of vaccine-treated lung

To analyze the effect of pertussis vaccine on the rat lung, we performed histological study on day 1 post-treatment. As shown in Fig. 3(E), SA-, PV-, PT-, and RE-treated lungs at day 1 demonstrated no significant changes in HE stained sections.

3.5. Quantification of toxicity-related genes

In the cluster analysis of lung, quite different genes were extracted on each 4 day (Table 2). Only five of the genes selected were in common, such as *S100A9* (NM_053587), *MCPT9* (NM_019323), *S100A8* (NM_053822), *CCL2* (M57441), and *MMP8* (NM_022221). These genes were thought to be strongly related to the toxicity of pertussis vaccine. Quantification analysis confirmed that 13 of the genes including *S100A9*, *MCPT9*, *S100A8*, *CCL2*, and *MMP8* at day 1 out of 25 array predicting transcripts demonstrated a good correlation between the microarray data and the quantitative gene expression data (Table 3 and Fig. 5A). When we performed the cluster analysis with these 13 genes, the cluster of RE- and PT-treated samples were clearly distinguished from SA- and PV-treated ones. Furthermore, the pattern of the dendrogram was similar to one with an array predicting 25 transcripts (Fig. 5B). In order to develop the gene expression detection system for pertussis vaccine toxicity using these 13 identified "genetic signatures", we applied the QuantiGene Plex assay with poly(A)+ RNA from the treated organs. As shown in Fig. 6, the results from the QuantiGene Plex showed good correlation with ones from Real-Time PCR analysis.

3.6. Quantitative detection of vaccine toxicity

Since it is difficult to prepare toxic vaccines for clinical use, we prepared samples containing various doses of RE vaccine (0.6–5.0 μg/ml) as a model of the accidental toxic vaccine. Three to five rats per group were analyzed at day 1 after sample administration. The lung lysates from the various sample-treated animals were assayed with QuantiGene Plex assay. As shown in Fig. 7, *S100A9*, *S100A8*, *MMP9*, *BEST5*, *MX2*, *IRF7*, *IFI27L*, *MMP8*, and *CYP2E1* were found to be suitable markers for RE vaccine toxicity. Expression of these nine genes was dependent on the dose of RE. On the other hand, *MCPT9*, *CCL2*, *IFIT3*, and *NGP_predicted* were not significantly altered with RE-treatment. These data correspond to that from poly(A)+ RNA (Fig. 6). Since these 13 "genetic signatures" can not only detect the toxicity of RE, but pertussis toxin as shown in Fig. 6, the assay system with the QuntiGene Plex should have the possibility to appropriately survey most pertussis vaccine toxicity and will become a new vaccine safety control method.

4. Discussion

Although whole-cell pertussis vaccine is effective to prevent whooping cough, it has caused local reactions such as redness, swelling, and pain at the injection site. However, little is known about the vaccine's comprehensive influences. In order to address this problem, we applied DNA microarray analysis and the quantification system of the specific gene expressions to analyze the vaccine's influence.

For DNA microarrays, we analyzed the gene expression profile in the liver, lung, kidney and brain from the treated rats, and selected the most suitable organ for the detection of vaccine toxicity. The

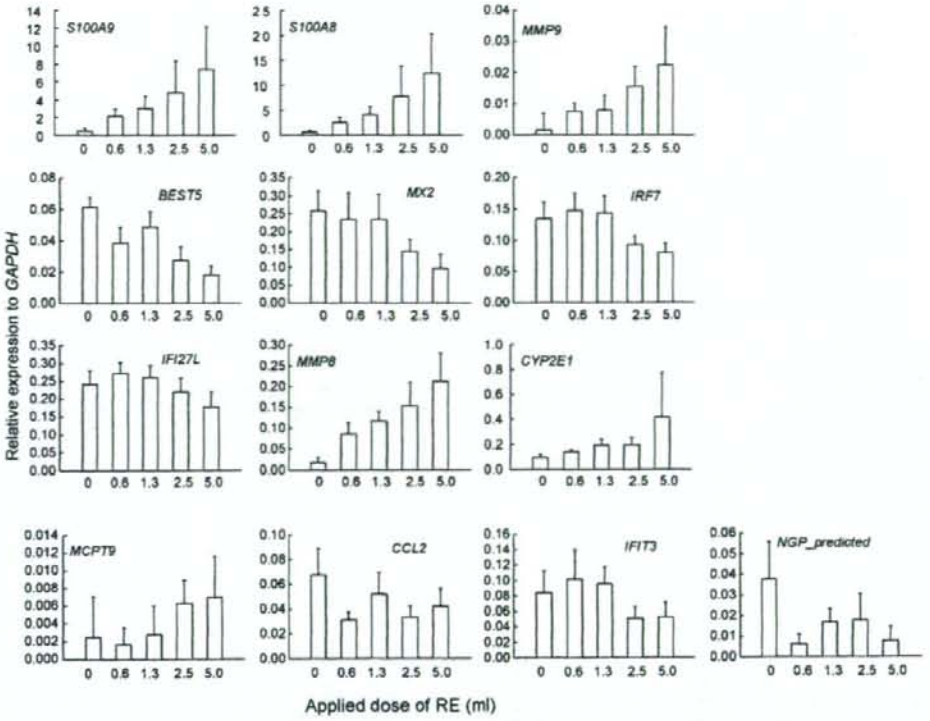

Fig. 7. Toxicity-related biomarkers of pertussis vaccine. SA- and various doses of RE-treated lung lysates were analyzed with QuantiGene Plex assay. Three to five animals for each sample were assayed by QuantiGene Plex in two experiments and shown as the mean expression ± S.D.

liver is thought to be one of the most appropriate organs to analyze the biological alteration with vaccine toxicity, because it is the major organ that metabolizes toxic agents. Moreover, many studies regarding pharmaceutical toxicity analysis in the liver using DNA microarray are ongoing [11]. In our previous study, we clarified the pertussis toxin-related genes by analyzing the expression profiles for RE-treated liver [12]. In this study, we performed clustering analysis for the vaccine or toxin treated tissues. However, the expression level of toxicity-related genes showed various in liver (Fig. 4A), kidney (Fig. 4B), and brain (Fig. 4C) depending on the sample treated animals. On the other hand, the lung genes which were extracted by DNA microarray classified the clusters sharply. Only sample #202 in Fig. 3 was miss-categorized in the wrong cluster. This sample was subsequently confirmed to be a technical accident. Besides sample #202, the clustering results of the lung are quite neat. From these results, we could recognize three important points regarding the lung samples. First, the data from two independents closely correspond to each other, meaning that the expression pattern in the lung is repeatable. Second, the clustering analysis showed clear categorization, meaning that the expression pattern of clustered PT- and RE-treated samples were strictly separated from that of SA- and PV-treated samples. Third, clear categorization was seen from day 1, meaning that the gene expression data was sensitive to detect vaccine effects. Furthermore, the clustering data from the lung was revealed to be reproducible. These results from the lung also demonstrated an interesting opinion that lung might be the most suitable organ for detecting the toxicity contained in pertussis vaccine using comprehensive microarray analysis.

Recently, McGuirk et al. elucidated the mechanisms involved in immune reactions between *B. pertussis* and pertussis vaccine in the lung, and a dramatic influx of neutrophils was observed in the lungs following *B. pertussis* infection of non-immunized mice [13]. Moreover, the inflammatory response was suppressed in the lungs of mice immunized with Th1-inducing killed-whole bacteria vaccine or Th2-inducing subunit vaccine [14]. These findings suggest that the functional responses and phenotype of local pulmonary T cells are generated by respiratory infection with *B. pertussis*, and the lung is a key organ, which functions as a protector for inflammatory responses. Other organs such as the kidney and brain did not show any clear clustering patterns by microarray analysis, meaning that of the four organs tested, the lung should be a feasible organ to analyze the expression pattern of toxicity-related genes in the case of pertussis vaccines.

Focused on the genes, which showed dramatically altered expression pattern in PT-treated samples compared with SA-treated ones in the lung (expression ratios over 0.75 in $\log_2$ scale on average ($P < 0.01$)), at day 1 post-administration, 25 transcripts were extracted to distinguish the individual samples. As shown in Figs. 3 and 4, RE- and PT-treated samples were sharply distinguished from SA- and PV-treated samples in lung, although brain, kidney, and liver samples did not have a similar contrast. In these 25 transcripts, the expression of 13 genes was correlated between the microarray data and Real-Time PCR data. These 13 "signatures" should be the predictive biomarkers of toxicant effect included in the vaccine. Using these signatures, we tried to develop more sensitive and more scientifically well-grounded methods for the quality control of vaccines.

Table 3
"Genetic signatures" for pertussis vaccine toxicity

Accession No.	Symbol	Category	Description	SA	PV	PT	RE
NM_053587	*S100a9*	Inflammation	A calcium binding protein that may be associated with acute inflammatory processes, coupled with S100a8	−1.40 ± 0.69	−0.98 ± 0.37	0.58 ± 0.40	2.84 ± 0.41
NM_019323	*Mcpt9*	Inflammation	A serine protease expressed in mast cells, but the precise function has not yet determined	−2.72 ± 0.30	−2.48 ± 0.27	0.57 ± 0.35	−1.58 ± 0.25
NM_053822	*S100a8*	Inflammation	May play a role in inflamatory responses such as cell motility, coupled with S100a9	−2.68 ± 0.67	−2.22 ± 0.46	−0.56 ± 0.54	2.14 ± 0.45
NM_031055	*Mmp9*	Peptidoglycan metabolism	Metalloproteinase involved in extracellular matrix remodeling, bone resorption, and immune responses	−2.21 ± 0.40	−2.25 ± 0.41	−1.30 ± 0.34	−0.35 ± 0.19
Y07704	*Best5*	Ossification	Induced by IFN and involved in bone formation	−0.22 ± 0.36	−0.36 ± 0.35	−1.03 ± 012	−1.37 ± 0.10
NM_017028	*Mx2*	Immune response	Involved in inhibiting vesicular stomatitis virus, but not an anti-influenza molecule	0.77 ± 0.30	0.72 ± 0.27	−0.33 ± 0.14	0.05 ± 0.25
XM_215121	*Irf7*	–	Unknown	0.81 ± 0.11	0.82 ± 0.16	0.04 ± 0.25	0.60 ± 0.21
NM_130743	*Ifi27l*	Immune response	Induced by steroid hormone, IFN and LPS in endometrium at implantation, dendric cells and macrophases	0.86 ± 0.35	0.36 ± 0.37	−0.02 ± 0.15	0.40 ± 0.23
NM_031530	*Ccl2*	Inflammation	A ligand for CCR2 that acts as a chemoattractant of monocytes	−0.09 ± 0.18	0.01 ± 0.10	1.12 ± 0.58	0.54 ± 0.39
XM_220059	*Ifit3*	Immune response	May induced by IFN or virus infection	2.42 ± 0.13	2.35 ± 0.48	1.20 ± 0.66	2.55 ± 0.39
NM_022221	*Mmp8*	Peptidoglycan metabolism	May play a role in appositional bone formation and regulation of the extracellular matrix	−0.23 ± 0.67	0.32 ± 0.24	2.04 ± 0.51	3.23 ± 0.45
J02627	*Cyp2e1*	Xenobiotic metabolism	Protects hepatocytes from stress-induced cell death	−4.03 ± 0.21	−3.93 ± 0.23	−3.25 ± 0.21	−0.71 ± 0.52
XM_236646	*Ngp_predicted*	–	Neutrophilic granule protein (predicted)	−3.38 ± 0.61	−3.04 ± 0.50	−1.33 ± 0.48	−3.04 ± 0.45

Cyanine 5-labeled lung RNA and Cyanine 3-labeled rat common reference RNA were competitively hybridized to microarrays. Hybridizaiton signals were processed into primary expression ratios ([Cyanine 5-intensity obtained from each sample]/[Cyanine 3-intensity obtained from common reference RNA]), and normalized (primary expression ratios). The primary expression ratios were converted into $\log_2$ values ($\log_2$ Cyanine 5-intensity/Cyanine 3-intensity) as described in Section 2. $\log_2$ values for each sample were taken an average and calculated S.D.

Of these 13 genes, five independent genes were universally selected throughout the testing periods, such as *S100A9* (NM_053587), *MCPT9* (NM_019323) *S100A8* (NM_053822), *CCL2* (M57441), and *MMP8* (NM_022221). Consistent with studies by McGuirk and colleagues, the five genes obtained from our microarray analysis are mainly associated with inflammatory or anti-inflammatory responses. S100A8 and S100A9 belong to the S100 protein family, which is characterized by the presence of two EF-hand type calcium-binding motifs [15]. They are mainly produced by phagocytes and form homo- and heterodimers in a calcium-dependent manner, causing neutrophil infiltration. Overexpression of these proteins were observed at local sites of inflammation, and elevated serum levels have been found along with a number of inflammatory disorders [16,17]. MCPT9 was cloned from a mucosal mast cell cDNA library in 1997 [18,19]. The expression of MCPT9 in connective tissue mast cells may be relatively low, but it is one of the major proteases in mucosal mast cell granules. It has a putative proteinase activity and apparently lacks tryptase, but the precise function of MCPT9 has not been elucidated. CCL2 is a member of the CC chemokine family involved in leukocyte physiology and trafficking. CCL2 mediates monocyte recruitment and entry into vessel walls. Overexpression of CCL2 led to atherosclerosis [20], and observed during the acute phase of several inflammatory disorders in human [20,21]. In a clinical study, the CCL2 level in plasma is accumulated along with lipid abnormalities [22]. MMP8 is one of the interstitial collagenases of the MMP family of extracellular and cell-surface associated, highly conserved zinc-dependent endopeptidases. MMP8 is mainly produced by neutrophils, and its collagenase activity is considered to correlate with neutrophil infiltration. In contrast, recent data from *MMP8-/-* mice in an asthma model showed increased neutrophilic and eosinophilic infiltration in the airway walls, indicating anti-inflammatory roles of MMP8 [23,24]. By accumulating the microarray-based information regarding vaccine treated samples, the mechanisms of vaccine toxicity will be elucidated genetically.

Although we identified 13 toxicity-related genes from the microarray analysis, it took a lot of effort to quantify all the genes by Real-Time PCR one by one. In order to quantify these genes in a convenient way, QuantiGene Plex assay was applied. QuantiGene Plex assay can deal with 13 genes in one reaction well. Furthermore, we can use the tissue lysate sample for the reactions instead of their purified RNAs, meaning that the assay avoids variation or errors resulting from extraction and amplification. Data for all 13 genes from QuantiGene Plex assay were closely correlated with the data from Real-Time PCR, and the quality was validated, as shown in Fig. 6. In Fig. 7, *S100A9*, *S100A8*, *MMP9*, *BEST5*, *MX2*, *IRF7*, *IFI27L*, *MMP8*, and *CYP2E1* were found to be suitable markers for RE vaccine toxicity. Furthermore, we confirmed that RE vaccine toxicity was measurable by means of the specific expression level of these nine genes in the lung lysate. The QuantiGene Plex assay has the advantages of the handling-convenience and the data-accuracy. For the new control test for vaccine toxicity, this assay will be one of the expecting candidates.

Some vaccines have been highly purified and their components crystallized, and their structures have been evaluated at the molecular level. However, we are still required to perform safety tests before the releasing the vaccine lots. Using the animal safety tests, we could detect severe weight loss, which was highly related to RE-treatment (Fig. 1), but the level of weight loss is not consistent between the tested animals. Histological studies with the treated-animals did not show any abnormal appearance in RE or PT treated lung sections (Fig. 3E). Conventional animal tests should be improved in many points. Nowadays, the four Rs, Replacement,

Reduction, Refinement, and Responsibility of animal experiments are advocated. To reduce the number of animals for safety tests and to refine the test's sensitivity, we are required to use the new vaccine evaluation system. Since the quantification of array-precipitated gene in this study is reproducible and objective, we think that it is possible to reduce the number of animals to confirm the safety of vaccines.

In this study, we focused on the pertussis vaccine. In the future, for the evaluation of all kinds of vaccines, this microarray analysis will play an important role as the new safety control test, especially for checking the toxin reactive transcripts. For another purpose of development of this vaccine-evaluation assay, we would utilize this for developing new vaccines. Nowadays, we are on the verge of a pandemic of high pathogenic influenza; therefore, new effective vaccines are urgently required. However, the evaluation of vaccine safety involves a long period of time to conduct tests and seek regulatory approval. In order to speed up vaccine production, we hope this assay would provide us with a strong tool for quicker development of new and effective vaccines.

References

[1] Sato H, Sato Y. *Bordetella pertussis* infection in mice: correlation of specific antibodies against two antigens, pertussis toxin, and filamentous hemagglutinin with mouse protectivity in an intracerebral or aerosol challenge system. Infect Immun 1984;46(November (2)):415–21.

[2] Atlanta G. Epidemiology and prevention of vaccine-preventable diseases. 8 ed. CDC, National Immunizing Program; 2000.

[3] Horiuchi Y, Takahashi M, Konda T, Ochiai M, Yamamoto A, Kataoka M, et al. Quality control of diphtheria tetanus acellular pertussis combined (DTaP) vaccines in Japan. Jpn J Infect Dis 2001;54(October (5)):167–80.

[4] Kurokawa M. Toxicity and toxicity testing of pertussis vaccine. Jpn J Med Sci Biol 1984;37(April (2)):41–81.

[5] Hamadeh HK, Bushel PR, Jayadev S, Martin K, DiSorbo O, Sieber S, et al. Gene expression analysis reveals chemical-specific profiles. Toxicol Sci 2002;67(June (2)):219–31.

[6] Ejiri N, Katayama K, Kiyosawa N, Baba Y, Doi K. Microarray analysis on Phase II drug metabolizing enzymes expression in pregnant rats after treatment with pregnenolone-16alpha-carbonitrile or phenobarbital. Exp Mol Pathol 2005;79(December (3)):272–7.

[7] Ministry of Health Welfare, J.G. The minimum requirements of biological products of Japan 1986. Tokyo: Ministry of Health and Welfare; 1986.

[8] Kobayashi S, Ito E, Honma R, Nojima Y, Shibuya M, Watanabe S, et al. Dynamic regulation of gene expression by the Flt-1 kinase and Matrigel in endothelial tubulogenesis. Genomics 2004;84(July (1)):185–92.

[9] Ito E, Honma R, Imai J, Azuma S, Kanno T, Mori S, et al. A tetraspanin-family protein, T-cell acute lymphoblastic leukemia-associated antigen 1, is induced by the Ewing's sarcoma-Wilms' tumor 1 fusion protein of desmoplastic small round-cell tumor. Am J Pathol 2003;163(December (6)):2165–72.

[10] Canales RD, Luo Y, Willey JC, Austermiller B, Barbacioru CC, Boysen C, et al. Evaluation of DNA microarray results with quantitative gene expression platforms. Nat Biotechnol 2006;24(September (9)):1115–22.

[11] Shipkova M, Spielbauer B, Voland A, Grone HJ, Armstrong VW, Oellerich M, et al. cDNA microarray analysis reveals new candidate genes possibly linked to side effects under mycophenolate mofetil therapy. Transplantation 2004;78(October (8)):1145–52.

[12] Hamaguchi I, Imai J, Momose H, Kawamura M, Mizukami T, Kato H, et al. Two vaccine toxicity-related genes Agp and Hpx could prove useful for pertussis vaccine safety control. Vaccine 2007;25(April (17)):3355–64.

[13] McGuirk P, Mahon BP, Griffin F, Mills KH. Compartmentalization of T cell responses following respiratory infection with *Bordetella pertussis*: hyporesponsiveness of lung T cells is associated with modulated expression of the co-stimulatory molecule CD28. Eur J Immunol 1998;28(January (1)):153–63.

[14] McGuirk P, Mills KH. A regulatory role for interleukin 4 in differential inflammatory responses in the lung following infection of mice primed with Th1- or Th2-inducing pertussis vaccines. Infect Immun 2000;68(March (3)):1383–90.

[15] Roth J, Vogl T, Sorg C, Sunderkotter C. Phagocyte-specific S100 proteins: a novel group of proinflammatory molecules. Trends Immunol 2003;24(April (4)):155–8.

[16] Bozinovski S, Cross M, Vlahos R, Jones JE, Hsuu K, Tessier PA, et al. S100A8 chemotactic protein is abundantly increased, but only a minor contributor to LPS-induced, steroid resistant neutrophilic lung inflammation in vivo. J Proteome Res 2005;4(January–February (1)):136–45.

[17] Yui S, Nakatani Y, Mikami M, Calprotectin. (S100A8/S100A9), an inflammatory protein complex from neutrophils with a broad apoptosis-inducing activity. Biol Pharm Bull 2003;26(June (6)):753–60.

[18] Lutzelschwab C, Pejler G, Aveskogh M, Hellman L. Secretory granule proteases in rat mast cells. Cloning of 10 different serine proteases and a carboxypeptidase A from various rat mast cell populations. J Exp Med 1997;185(January (1)):13–29.

[19] Hunt JE, Friend DS, Gurish MF, Feyfant E, Sali A, Huang C, et al. Mouse mast cell protease 9, a novel member of the chromosome 14 family of serine proteases that is selectively expressed in uterine mast cells. J Biol Chem 1997;272(November (46)):29158–66.

[20] Aiello RJ, Bourassa PA, Lindsey S, Weng W, Natoli E, Rollins BJ, et al. Monocyte chemoattractant protein-1 accelerates atherosclerosis in apolipoprotein E-deficient mice. Arterioscler Thromb Vasc Biol 1999;19(June (6)):1518–25.

[21] Matsumori A, Furukawa Y, Hashimoto T, Yoshida A, Ono K, Shioi T, et al. Plasma levels of the monocyte chemotactic and activating factor/monocyte chemoattractant protein-1 are elevated in patients with acute myocardial infarction. J Mol Cell Cardiol 1997;29(January (1)):419–23.

[22] Kowalski J, Okopien B, Madej A, Makowiecka K, Zielinski M, Kalina Z, et al. Levels of sICAM-1, sVCAM-1 and MCP-1 in patients with hyperlipoproteinemia IIa and -IIb. Int J Clin Pharmacol Ther 2001;39(February (2)):48–52.

[23] Owen CA, Hu Z, Lopez-Otin C, Shapiro SD. Membrane-bound matrix metalloproteinase-8 on activated polymorphonuclear cells is a potent, tissue inhibitor of metalloproteinase-resistant collagenase and serpinase. J Immunol 2004;172(June (12)):7791–803.

[24] Gueders MM, Balbin M, Rocks N, Foidart JM, Gosset P, Louis R, et al. Matrix metalloproteinase-8 deficiency promotes granulocytic allergen-induced airway inflammation. J Immunol 2005;175(August (4)):2589–97.

Vaccine (2008) 26, 2270–2283

available at www.sciencedirect.com

ScienceDirect

journal homepage: www.elsevier.com/locate/vaccine

Application of DNA microarray technology to influenza A/Vietnam/1194/2004 (H5N1) vaccine safety evaluation

Takuo Mizukami[a,1], Jun-ichi Imai[b,1], Isao Hamaguchi[a,1], Mika Kawamura[b,c], Haruka Momose[a], Seishiro Naito[a], Jun-ichi Maeyama[a], Atsuko Masumi[a], Madoka Kuramitsu[a], Kazuya Takizawa[a], Nobuo Nomura[d], Shinya Watanabe[b], Kazunari Yamaguchi[a,*]

[a] *Department of Safety Research on Blood and Biological Products, National Institute of Infectious Diseases, 4-7-1 Gakuen, Musashimurayama, Tokyo 208-0011, Japan*
[b] *Department of Clinical Informatics, Tokyo Medical and Dental University, Tokyo, Japan*
[c] *Medicrome, Inc., Tokyo, Japan*
[d] *Biological Information Research Center, National Institute of Advanced Industrial Science and Technology, Japan*

Received 18 August 2007; received in revised form 11 December 2007; accepted 8 February 2008
Available online 3 March 2008

KEYWORDS
Influenza vaccine;
Pandemic;
H5N1;
DNA microarray;
Safety test

Summary We propose that cDNA microarray analysis can be used in the quality control of pandemic and endemic influenza vaccine. Based on the expression profiles of 76 genes in the rat lung one day after inoculation of influenza vaccine, we can distinguish whole-virion influenza vaccine (PDv: pandemic influenza vaccine and WPv: whole virion-particle vaccine) and subvirion vaccine (HA vaccine) from saline. Among these 76 genes, we found genes up-regulated by influenza infection, as well as genes involved in the immune response, and interferon. Hierarchical clustering of each influenza vaccine by the expression profiles of these 76 genes matched data from current quality control tests in Japan, such as the abnormal toxicity test (ATT) and the leukopenic toxicity test (LTT). Thus, it can be concluded that cDNA microarray technology is an informative, rapid and highly sensitive method with which to evaluate the quality of influenza vaccines. Using DNA microarray system, consistent with the results of the ATT and LTT, it was clarified that there was no difference in vaccine quality between PDv and WPv.

Introduction

Influenza virus triggers a highly contagious acute respiratory illness, which can lead to high fever, muscle aches, sore throat, non-productive cough, and sometimes lead to death.

* Corresponding author. Tel.: +81 42 561 0771.
E-mail address: kyama@nih.go.jp (K. Yamaguchi).
[1] These authors contributed equally to this work.

0264-410X/$ – see front matter © 2008 Elsevier Ltd. All rights reserved.
doi:10.1016/j.vaccine.2008.02.031